Journal of Sedimentary Environments
https://doi.org/10.1007/s43217-024-00192-8

RESEARCH

Tracing the Late Permian Gondwana surface environments using sedimentary biomarkers from the Raniganj Formation, Damodar Valley, Eastern India

Nihar Ranjan Kar[1,2] · Devleena Mani[1] · E. V. S. S. K. Babu[2]

Received: 19 February 2024 / Revised: 30 June 2024 / Accepted: 2 July 2024

Abstract
Sedimentary biomarkers are useful proxies for determining the source rock properties and its paleo-environmental conditions of deposition. The Upper Permian shales of the Raniganj Formation in the Jharia sub-basin of the Damodar Valley were analyzed for their biomarker distribution patterns using gas chromatography–mass spectrometry, with the aim to decipher the Late Permian Gondwana surface environment, organic provenance and source rock properties, including the thermal maturity. The shales are characterized by acyclic isoprenoids, *n*-alkane distributions ranging between nC_{12} to nC_{35} with no odd–even predominance, hopanes, steranes and polyaromatic hydrocarbons. The organic-matter input, primarily from terrestrial Type-III kerogen, got deposited in open water or swampy environments. Stratigraphically, a shift in the depositional environment from marine/aquatic to terrestrial was marked from the depth to the top of the Raniganj Formation. This leads to the inference of a geographic location close to or along the shoreline, potentially within a peri-tidal environment, where sedimentation was influenced significantly by waves. The organic-rich shales are thermally mature in the oil-generation stage and exhibit increasing maturity with depth but have not undergone sufficient burial for the gas generation. Overall, there is a combination of organic-matter inputs, from both terrestrial and aquatic sources, along with a discernible transition in the depositional environment from marine/aquatic to terrestrial in the area, leading to deposition of organically rich and thermally mature Raniganj shales.

Keywords Source rock · Raniganj Formation · Gondwana basin · Depositional environment · Permian shales · Biomarker

1 Introduction

The Gondwana basins of the world, which once formed the part of the Supercontinent Gondwanaland, are characterized by distinct spatial arrangements and temporal similarities in their floral, faunal, and lithologic distribution (Mukhopadhyay et al., 2010). The Gondwana was a large continent with a crustal area of more than 100×10^6 km^2 (Parrish, 1990). Globally, the Gondwana formations retain a diverse array of depositional traits, reflecting a range of ancient climatic conditions such as glaciation, river-based sedimentation, occasional marine incursions, warm spells, and humid periods. Abundant plant fossils with sporadic findings of both vertebrate and invertebrate fossils, characterize the Gondwana formations. The latitudinal position of the continent, sea level variations, tectonics, and climate influenced the paleo and depositional environment throughout the Gondwana time (Parrish, 1990).

In India, the Gondwana basins are arranged in a linear pattern along the suture zones between the Precambrian cratonic blocks of the Indian Shield. These basins primarily contain continental rift sediments, occasionally augmented by limited marine contributions (Mukhopadhyay et al., 2010). The deposition of Gondwana sediments took place mainly in three river valley basins: Damodar, Son-Mahanadi, and Pranhita–Godavari (Fig. 1; Roy & Purohit, 2018). The Gondwana Supergroup is divided into two

Communicated by M. V. Alves Martins

✉ Devleena Mani
dtiwarisp@uohyd.ac.in

[1] Center for Earth, Ocean and Atmospheric Sciences (CEOAS), University of Hyderabad, Gachibowli, Hyderabad, Telangana 500046, India

[2] Council of Scientific and Industrial Research–National Geophysical Research Institute, Uppal Road, Habsiguda, Hyderabad, Telangana 500007, India

Published online: 20 July 2024

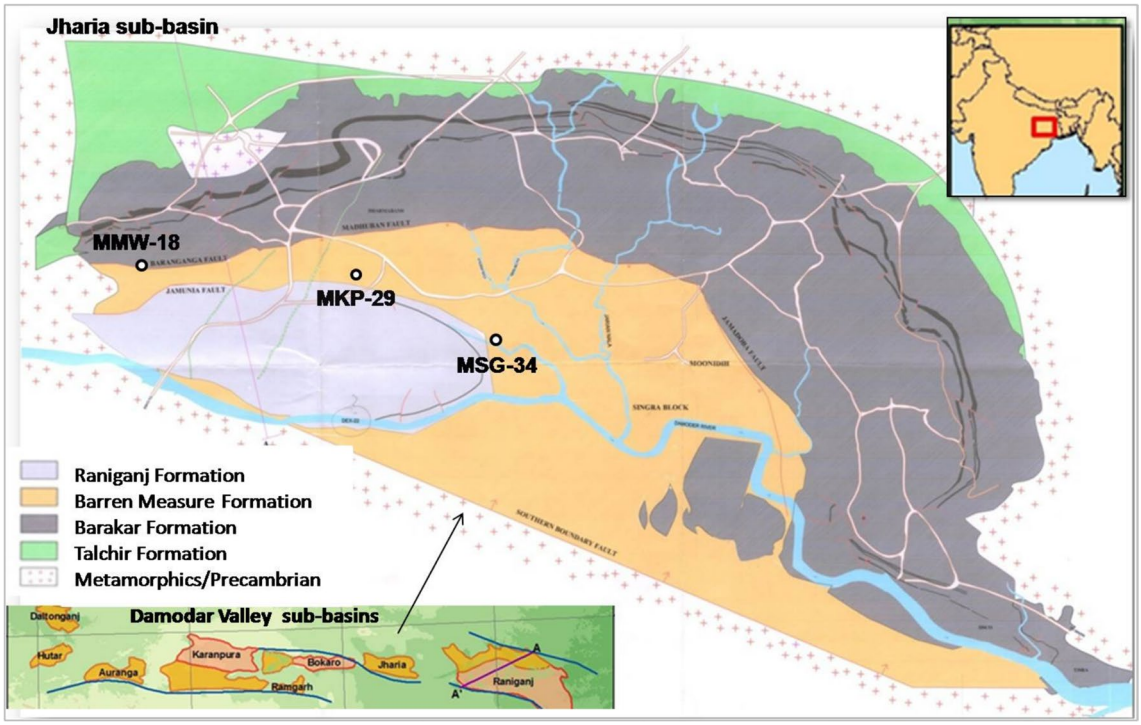

Fig. 1 Geologic map of Jharia sub-basin in the background of the Damodar Valley sub-basins, located in the Northeastern India (modified after Chandra, 1992; Mani et al., 2015)

main divisions. The Lower Gondwana Group, dating to the Permo-Carboniferous Period, is identified by its distinctive flora consisting of Gangomopteris, Glossopteris, and Dicrodium species (Mukhopadhyay et al., 2010). The Upper Gondwana Group from the Mesozoic Era is characterized by a different flora, featuring Lepidopteris and Ptilophyllum (Mukhopadhyay et al., 2010). Stratigraphically, the glaciomarine Talchir Formation is the oldest, followed by the overlying Karharbari, Barakar, Barren Measures, and Raniganj Formations (Mukhopadhyay et al., 2010). More than 5-km thick fossiliferous sedimentary successions of these formations bear distinct flora and fauna of the time, including extensive coal seams, except for the Barren Measures. Primary coal-bearing formations within the basins include the Lower Gondwana Karharbari and Barakar and the Upper Gondwana Raniganj and its equivalents. The presence of marine/lacustrine sedimentary layers sandwiched between the continental depositions led to the formation of the coal-free Barren Measures Formation, which is suggested to be deposited in an off-shore shelf, wave- or river-dominated delta mouth, or delta plain environments of either a marine or large lacustrine basin (Dasgupta, 2005; Roy, 2015). The depositional conditions of the Karharbari, Barakar, and Raniganj Formations indicate an origin distinct from that found in the Barren Measures. The lower Barakar Formation developed in mixed facies environment, with alternating wet and dry conditions, while the middle and upper Barakar Formations, along with the Raniganj coals, originated in wet forest swamps in a warm and humid climate (Mishra & Cook, 1992). In contrast, the Barren Measures Formation indicates an origin associated with lacustrine or marine conditions (Mani et al., 2015). The Raniganj coals exhibit a predominance of vitrinite, accompanied by significant proportions of both inertinite and exinite (Mishra & Cook, 1992). There are indications of potential marine influences or incursions reported by Gupta (1991, 1992) in the Ramgarh coalfield, Mukhopadhyay (1996) in South Karanpura, and in the West Bokaro coalfields by Chandra (1992). However, these observations are restricted to limited evidences and need further investigation (Gupta, 1999). The presence of extensive organic-rich and thermally mature shales among these major coal-bearing formations also makes this area a source of gaseous hydrocarbons within the basin (Mani et al., 2015). With shale rocks and oil shales becoming increasingly important as natural gas and petroleum resource in recent times, understanding the source rock properties, surface environment dynamics and depositional settings of these formations is important.

Sedimentary biomarkers, which are fossilized molecules derived from once living organisms, serve as a reliable proxy for characterizing the paleo-vegetation contribution and depositional environments (Mani et al., 2022). Distinct paleoenvironments, such as river valleys, deltas, and lakes were shaped by localized physical processes, while broader

global paleoclimatic patterns, influenced by oceanic and atmospheric currents, played a critical role in governing the distribution of flora and fauna, albeit on a larger scale (Raymond et al., 1985). Sedimentary biomarkers have improved the knowledge about precursor organisms and their habitable environments in several aspects, including the reconstruction of source organic input, redox, deposition, and preservation conditions, besides being helpful in various facets of hydrocarbon exploration. Due to their limited susceptibility to microbial and diagenetic degradation, biomarkers, especially *n*-alkanes, have the capability to preserve a wide range of information pertaining to the depositional history and origin of organic matter in the rock. In addition, several biomarker ratios, such as the carbon preference index (CPI), nor-neohopanes, steranes and polycyclic aromatic hydrocarbons (PAH's) yield insights into the thermal maturity of organic matter (Wakeham et al., 1980; Radke et al., 1982; Alexander et al., 1985, 1986, 1992; Mani & Kar, 2024).

This study presents discrete sedimentary biomarker distribution profiles obtained from drilled cores of carbonaceous shales from the Raniganj Formation in the Jharia sub-basin of the Damodar Valley, Eastern India, with the objective of deciphering the Late Permian Gondwana depositional environment, paleo-vegetation input and properties of organic matter, including the thermal maturity. The alkane, hopane and sterane markers along with the PAH's, determined using gas chromatography–mass spectrometry, reveal the shifts and variations in the Lower Gondwana depositional environment and the possible continental-marine transition, while providing significant constraints on the shale's source rock potential.

2 Geologic settings and stratigraphy

The Indian Gondwana basins are distributed across four major basin belts, namely, the (1) Trans-Indian basin belt, encompassing the ENE-WSW trending Satpura and Son Valley Basins, as well as the E-W to WNW-ESE trending Damodar-Koel Valley Basins; (2) Wardha-Pranhita–Godavari Valley Basin belt, which trends NNW-SSE; (3) Mahanadi Valley Basin belt, initially following a NW–SE trajectory but veering toward a WNW-ESE direction in the southernmost Talchir coalfield; and the (4) Purnea-Rajmahal-Galsi basin belt, which exhibits a NNW-SSE trending orientation (Fig. 1; Veevers & Tiwari, 1995; Mukhopadhya et al., 2010). Damodar Valley forms a part of the E-W trending Satpura-Damodar belt and comprises a series of E-W trending sub-basins (Fig. 1). These belts have mostly been formed as a result of the deposition of sediments in river valleys. The Damodar Valley Basin derives its name from the Damodar River, which traverses the Raniganj, Jharia, and Bokaro Sub-Basins and stands out as one of the most expansive and well-developed subdivisions within the Gondwana system (Fig. 1). This region boasts a wealth of diverse mineral resources, with a notable abundance of coal and mica. Rocks ranging in age from Archaean to Recent are present in the Damodar Valley Basin (Chandra, 1992). In most places, the Archean crystalline formations and Gondwana deposits have been intersected by post-Gondwana intrusions, with extensive multi-directional faults and lineaments punctuating the landscape. The Phanerozoic sedimentation atop the Neoproterozoic basement commenced with the deposition of Late Carboniferous Gondwana sediments. The sedimentary fill in this basin, measuring approximately 5300 m in thickness, consists of a Gondwana sequence spanning from the Permian Lower Gondwana Group, (approximately 2300 m), to the Triassic to Lower Cretaceous Upper Gondwana Group, (approximately 3000 m) (Krishnan, 1949; Mukhopadhyay et al., 2010). Sedimentation in the Damodar Basin initially occurred in the Late Carboniferous within sag-type basins, situated above the Precambrian basement, as a result of multiple deglaciations (Chandra, 1992). The basin experienced a significant transgressive event that resulted in widespread inundation, as indicated by the presence of marine fossils found in the uppermost layers of the Talchir Formation. These layers are characterized by a basal boulder bed and striation marks left by glaciers. In the deeper sections of the basin, conditions resembling a marine environment were prevalent during the deposition of the lower portion of the Barakar Formation. Following this phase, a regressive period ensued, during which the coal-bearing strata of the Barakar Formation were laid down in a tectono-sedimentary environment (Krishnan, 1949). The environment conducive to coal formation re-emerged during the subsequent regressive phase, coinciding with the deposition of the Raniganj Formation and its equivalents (Casshyap, 1970; Casshyap & Kumar, 1987; Casshyap & Tiwari, 1987). In the Cretaceous Period, there was an eruption of tholeiitic lava as Rajmahal Traps, accompanied by the emplacement of lamprophyre dikes and sills in the eastern part of the basin (Ghosh & Mukhopadhyay, 1985). The Jharia Sub-Basin has an NW–SE linear trend and is located between the Bokaro and Raniganj sub-basin toward the eastern part of the Damodar valley. In Jharia, the earliest Gondwana geologic unit is the Talchir Formation (Table 1). This formation directly underlies the Precambrian metamorphic rocks and is sequentially followed by the Barakar, Barren Measures, and Raniganj Formations. Generalized stratigraphic information about these geologic formations is presented in Table 1. The Barakar and Raniganj Formations emerge as the predominant coal-bearing layers. In contrast, the Barren Measures, positioned between the Barakar and Raniganj Formations, is characterized as a unit devoid of coal resources. Raniganj Formation, the topmost unit of the Lower Gondwana Group, has a thick succession of

Table 1 Litho-stratigraphy of Jharia sub-basin, Damodar Valley (modified after Chandra, 1992; Mani et al., 2015)

Age	Group	Formation	Litho-Type	Maximum thickness
Recent and sub-recent		Weathered	Alluvium, sandy clay, gravel etc	30 m
Unconformity				
Jurassic		Deccan Trap & other Igneous Intrusives	Dolerite dykes, Mica lamprophyre dyke & sills	
Unconformity				
Upper permian	DAMUDA	Raniganj	Fine grained feldspathic sandstones, Shale with coal seam	800 m
Middle permian		Barren Measure	Buff colored sandstone, shales and carbonaceous shales	730 m
Lower permian		Barakar	Buff colored coarse to medium grained feldspathic sandstones, grits, shales, carbonaceous shales and coal seam	+1250
Upper carboniferous		Talchir	Greenish shale and fine grained sandstones	245 m
Unconformity				
Archeans	Metamorphics			

fine-grained feldspathic sandstones, shales and coal. The Raniganj Series shows a regressive phase of coal-bearing formation (Casshyap, 1970; Casshyap & Kumar, 1987; Casshyap & Tiwari, 1987) in transition to the lower Barren Measures Formation (Table 1).

3 Materials and methods

Subsurface drilled shale cores from the West Mahuda block within the Jharia sub-basin (Fig. 1) were studied for their biomarker distributions. The water-based drilling mud residues were removed from the shales by rigorous washing with Type I Laboratory water, following which the samples were air-dried at room temperature. The uniformly powdered samples were then used to extract the organic matter.

3.1 Solvent extraction of organic matter

The organic matter from the shale samples was extracted using a Buchi Speed Extractor E-914. Solvent extraction of organic compounds from the powdered shale samples was done at elevated temperature (100 °C) and pressure (100 bar) using a 9:1 DCM:MeOH (dichloromethane and methanol) mixture (Table 2). The shale samples, weighing about 4 g were mixed with diatomaceous earth in an 80-ml extraction cell. Recovery standard, *n*-hexatriacontane-d_{74} (*n*-$C_{36}D_{74}$; 4 ml of 250 ppm), was added to the sample and a three-step extraction program was run to obtain the total lipid extract (TLE). The extracted organic matter (EOM) was concentrated to about 2–3 ml using multivapour. This mixture was completely dried under the gentle flow of nitrogen. Approximately 3 µl of DCM:MeOH (93:7 *v*/*v*) solvent was used for dissolving each milligram of EOM. Following this, *n*-pentane was added in a volume that was 40 times in excess of the combined EOM and DCM:MeOH mixture to remove the asphaltene fraction. Sulfur was then removed from the obtained maltene fraction by adding activated (HCl treated) copper.

Table 2 Extraction parameters for parallel and sequential pressurized liquid extraction of the organic matter from the shales of Jharia sub-basin, Damodar Valley

Parameter	Value
Solvent (DCM:Methanol)	9:1
Temperature	100 °C
Pressure	100 bar
Cells	80 ml
Cycles	3
Extraction time (static)	1 h; 5 min (hold time)
Discharge	4 min/3 min (1st/2nd/3rd cycle)
Flush/purge time	3 min solvent/5 min N_2

3.2 Column chromatography

Separation of the aliphatic, aromatic and polar fractions was achieved through the process of silica gel column chromatography. A burette of 30 cm length and 2 cm diameter, filled with 10 cm silica gel 60 (70-230 mesh) was taken, above which 1.5 cm of alumina was added. The EOM, mixed with alumina, was placed on the top of silica column. The separation process involved using 100 ml of hexane to elute the aliphatic fraction and a 150 ml mixture of hexane and DCM (1:4) to elute the aromatic fraction. Subsequently, the solvent fractions containing the analytes were concentrated to a volume of about 0.5–1 ml, while gently passing nitrogen gas over them. To facilitate the quantification of the target analytes, internal standards were added. Specifically,

deuterated androstane and deuterated tetracosane were added to the aliphatic fraction, while d2C_{27}ααα (20R)-cholestane was used for steranes, and d10-naphthalene were incorporated into the aromatic fraction.

3.3 Gas chromatography–mass spectrometry (GC–MS)

The analysis of the aliphatic fractions was conducted using a Varian 3800 GC coupled to a 320 Triple Quad Mass Spectrometer. The system was equipped with a DB-1 ms (100% Dimethylpolysiloxane) capillary column (60 m length × 0.25 mm inner diameter × 0.25 µm film thickness), made of fused silica. Helium, with a purity of 99.999%, was used as the carrier gas, with a constant flow rate of 1.2 ml/min. The injector port temperature was held steady at 300 °C. The MS transfer line and ion source were both configured at temperatures of 310 °C and 200 °C, respectively. The mass spectrometer operated in electron impact ionization (EI) mode at an energy level of 70 eV. The temperature of the GC column oven was initially set at 35 °C and held for 1 min. Subsequently, it was ramped up at a rate of 10 °C/min to reach 130 °C. Afterward, the temperature was further increased at a rate of 4 °C/min, until it reached 310 °C, where it was held constant for a duration of 10 min. Using an autosampler, a 1 µl sample injection was done in splitless mode. The GC–MS system was run in full scan mode, encompassing a mass range (*m*/*z*) of 50–600 amu. To identify compounds, a comparison was made between the GC-retention times, fragmentation patterns, and the *m*/*z* peaks of molecular ions in the samples and those found in biomarker standards sourced from CHIRON AS, Norway, the Norwegian Geochemical Standard- Jet Rock (NGS JR-1), as well as published mass spectra (b; Peters & Moldowan, 1993; Philp, 1985a). For aliphatic hydrocarbon fraction, in particular, an alkane standard, S-4106-100-HX *n*-alkane C_{10}–C_{40} (even + pristane and phytane) from CHIRON AS was used, and the *n*-alkanes were identified from *m*/*z* 57 chromatograms. The C_{19}–C_{24} tricyclic terpanes, pentacyclic triterpanes were identified from the characteristic *m*/*z* 191 along with the 370, 398, 412, and 426 molecular ions for C_{27}, C_{29}, C_{30} and C_{31} homologs, respectively. C_{27}–C_{30} sterane homologous were quantified by measuring peak areas in the *m*/*z* 217 chromatograms.

Four samples of Raniganj shales were taken for aromatic analysis. For the analyses of PAHs, the GC oven was programmed with initial temperature of 60 °C with a 1-min hold, followed a three-stage ramping process. First, it was raised to 175 °C at a rate of 6 °C/min with a 4-min hold, second to 235 °C at a rate of 3 °C/min with a 4-mine hold, and finally to 300 °C at a rate of 5 °C/min, where it was held for 15 min. The GC–MS system was operated in full scan mode in mass range from *m*/*z* 50 to 600 amu. The identification of methyl, dimethyl, and trimethyl naphthalenes was based on their respective chromatograms at *m*/*z* 142, 156, and 170, respectively. Similarly, phenanthrene, dibenzothiophene, as well as methyl and dimethyl phenanthrenes were identified using the chromatograms at *m*/*z* 178, 184, 192, and 206, respectively. These individual peaks were confirmed through comparison with existing literature data (George et al., 1998; Radke, 1987) and by referencing a comprehensive mass spectra library (NIST). Quantification was accomplished by comparing the peak areas of the target compounds with those of a known concentration of the internal standard anthracene-d10. Method blanks were performed to check for the presence of any trace organic contaminants from the laboratory and were found to be negligible. The recovery of deuterated hexatriacontane added prior to extraction in the powdered shale samples ranged from 80 to 85%. The EOM yield varied between 4 and 96 mg/g dry weight of the respective shale sample.

4 Result and discussions

The organic richness, kerogen type, and thermal maturity of sedimentary organic matter defines its effectiveness as source rocks in any basin. The Permian shales from the Raniganj Formation of the Jharia Sub-basin have been characterized to possess high TOC (3.40–23.09 wt%), with heterogeneous Type-III Kerogen and Tmax between 442 and 461 °C, suggesting a mature stage (oil window) for hydrocarbon generation (Mani et al., 2015). The maceral analysis of these reveals a dominance of vitrinite over liptinite and inertinite, with %VRo in a range of 0.99–1.29 (Mani et al., 2015). This is also corroborated by the Tmax (°C), and hydrogen indices (HI in mg HC/g TOC), implying largely Type-III kerogen in oil zone field maturity (Mani et al., 2015). Sedimentary biomarkers, studied here, provide significant insight on the depositional environment of these Upper Permian shales.

4.1 *n*-Alkanes and isoprenoids

The GC–MS traces of the extracted OM from shales exhibited significant concentrations of the saturated hydrocarbons, spanning from alkanes (nC_{12} to nC_{35}), hopanes and steranes, as well as acyclic isoprenoids. The distribution of *n*-alkanes, in general, is unimodal with no significant odd over even predominance. The peak maxima is shown by nC_{17}-pristane range (Fig. 2). The *n*-alkane profile maxima can reveal if a source interval is largely originated from marine or terrestrial organic matter, as well as whether the bitumen is thermally mature or not (Gonzalez-Vila, 1995; Peters et al., 2005). Long-chain *n*-alkanes with odd carbon numbers (> C_{27}) are commonly found in terrestrial vegetation (Eglinton & Hamilton, 1967; Egüez et al., 2022). Submerged and

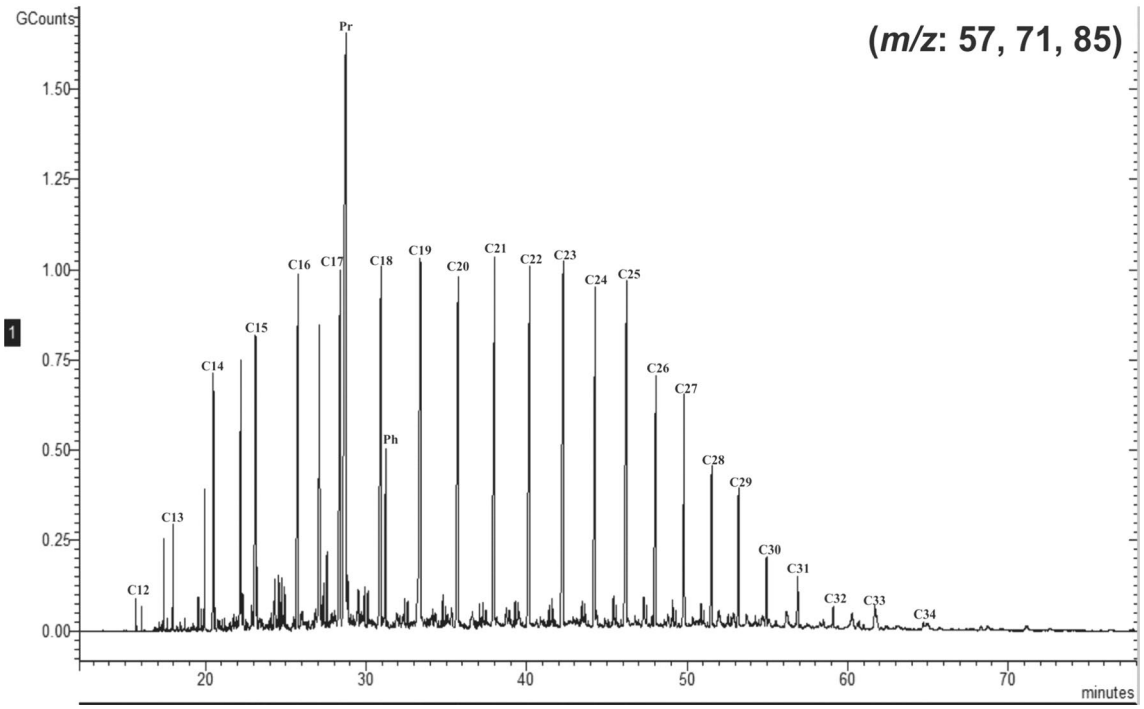

Fig. 2 Representative *n*-alkane spectra of R-4 (*m/z* 57, 71, 85) of the extracted organic matter from the shales of Raniganj Formation of Jharia Sub-basin, Damoder valley basin

floating aquatic macrophytes are characterized by mid-chain homologues in the C_{21}–C_{25} range (Barnes & Barnes, 1978; Cranwell, 1981; Ficken et al., 2000; Egüez et al., 2022). Short-chain homologues, specifically *n*-alkanes in the C_{17}–C_{21} range, are associated with aquatic algae, mosses, ferns (Cranwell et al., 1987), and microbial organisms (Eckmeier & Wiesenberg, 2009; Egüez et al., 2022). The alkane abundance from studied shales shows dominance of C_{16}–C_{25} peaks, probably sourced from aquatic organic matter, and accompanied with microbial action. The origin and maturity level of organic matter have a notable impact on the predominance of odd and even carbon numbers within hydrocarbon compounds (Tissot & Welte, 1984). The Carbon Preference Index (CPI) is a ratio calculated by dividing the sum of odd-carbon-numbered alkanes by the sum of even-carbon-numbered alkanes (Peters et al., 2005). The examined shales have a CPI value of between 0.8 and 1.5 (avg. > 1), with neither even nor odd carbon preference (Table 3; Fig. 3).

The pristane–phytane ratio (Pr/Ph) values of the sedimentary rocks are widely used as indicators for various depositional settings (Didyk et al., 1978; Peters et al., 2005). This ratio provides valuable insights into environmental conditions, considering the diverse processes involved in pristane and phytane formation. The ratio mirrors the oxidative pathway responsible for pristane formation from the chlorophyll phytyl side-chain, as opposed to the multiple reductive pathways leading to phytane (Didyk et al., 1978; Rontani & Bonin, 2011). Pr/Ph ratios (> 3) suggest contribution of terrestrial organic matter from higher plants that has been oxidized before preservation (Powell, 1984). Low Pr/Ph values (typically < 2), are indicative of aquatic depositional environments such as marine, fresh, and brackish water settings characterized by reducing conditions. Intermediate values (2–4) suggest fluvio-marine and coastal swamp environments. Very high Pr/Ph values (up to 10) are associated with peat swamp-type depositional environments, where extensive oxidation of organic matter has occurred (Limbach, 1975). The Raniganj shales exhibits a Pr/Ph ratio ranging from 2 to 6 (Fig. 3), suggesting a redox condition associated with deposition in a fluvio-marine or coastal swamp setting.

Isoprenoid/*n*-alkane ratios serve as valuable indicators for evaluating the thermal maturity of non-biodegraded oils and bitumens. Source rocks deposited under alternating circumstances between swamps and open waterways are indicated by Pr/*n*-C_{17} ratios ranging from 0.5 to 1.0 (Lijmbach, 1975). Except for R-1 and R-4, all other Raniganj samples have Pr/nC_{17} ratios of < 1.0, suggesting a primarily marshy to open water habitat. Similarly, the correlation between Pr/nC_{17} verses Ph/nC_{18} shows that the Raniganj shales lie in field of type-III kerogen of terrigenous origin, with oxic depositional environment (Fig. 4).

The P_{aq} proxy ratio, where, $P_{aq} = (nC_{23} + nC_{25})/(nC_{23} + nC_{25} + nC_{29} + nC_{31})$, suggests the type of macrophytes input from the terrestrial organic matter. The

Table 3 Important *n*-alkane biomarker ratios from the Raniganj Formation, Damodar Valley Basin

Ratios	R-1	R-2	R-3	R-4	R-5	R-6	R-7	R-8	R-9
	n-alkane and isoprenoids (*m/z*: 57, 71, 85)								
Pr/Ph	4.65	6.15	3.34	6.3	3.71	2.93	4.64	5.39	4.19
Pr/nC_{17}	1.38	0.95	0.36	3.16	0.54	0.35	0.34	0.49	0.28
Ph/nC_{18}	0.26	0.14	0.23	0.4	0.11	0.1	0.08	0.09	0.06
nC_{25}/nC_{18}	0.7	0.81	0.31	0.87	0.54	0.52	0.66	0.26	0.4
CPI	1.31	1.55	1.38	1.3	1.14	1.21	1.09	0.82	1.19
TAR	0.71	0.42	0.3	0.42	0.33	0.29	0.24	0.27	0.17
TMD	0.61	0.47	0.33	0.44	0.36	0.32	0.34	0.23	0.23
Paq	0.82	0.83	0.71	0.86	0.82	0.82	0.77	0.81	0.86
$(Pr+nC_{17})/(Ph+nC_{18})$	1.64	1.54	2.33	2.34	1	1	1.23	1.34	1
	Hopanes (*m/z*: 191)								
Ts/(Ts + Tm)	0.09	0.12	0.13	0.08	0.24	0.5	0.55	0.74	0.75
C_{29}hopane/C_{30}hopane	0.77	0.5	0	0.64	0.45	0.43	0.33	0.25	0
C_{31} 22S/(22S + 22R)	0.55	0.59	0.59	0.48	0.52	0.55	0.57	0.53	0.56
$\%(C_{19}+C_{20})$ TT	79.76	72.68	92.55	80.29	61.39	50.25	76.2	77.12	75.27
$\%C_{21}$ TT	9.92	16.54	3.38	10.66	19.38	26.78	12.06	10.96	11.77
$\%C_{23}$ TT	10.33	10.79	4.09	9.07	19.24	22.99	11.76	11.94	12.98
$C_{30}D/C_{29}Ts$	0.16	0.12	0.12	0.11	0.29	1.1	1.19	1.78	1.97
C_{21}/C_{20}	0.53	0.38	0.05	0.32	0.71	1.05	0.4	0.32	0.34
C_{23}/C_{21}	1.05	0.66	1.21	0.86	1	0.86	0.98	1.09	1.11
	Steranes (*m/z*: 217)								
C_{29} 20S/(20S + 20R)	0.56	0.6	0.58	0.49	0.53	0.54	0.56	0.52	0.55
C_{29} ββ/(ββ + αα)	0.59	0.6	0.57	0.46	0.53	0.53	0.55	0.54	0.54
$\%C_{27}$	20.27	22.5	22.25	12.92	26.79	36.94	23.6	23.86	22.64
$\%C_{28}$	20.12	22.41	22.14	18.31	22.47	21.93	23.59	23.47	24.55
$\%C_{29}$	59.63	55.11	55.62	68.78	50.75	41.14	52.82	52.69	52.83

values < 1 suggest non-emergent plant matter input, 0.1–0.4 suggests emergent macrophytes and 0.4–1 suggests submerged/floating macrophytes (Ficken et al., 2000). The P_{aq} ratio of the Raniganj samples lies in the range of 0.7–0.8 (Table 3; Fig. 3), suggesting a submerged/floating macrophytes type terrestrial organic matter. However, there is a notable variation in the ratios, depicting changes in macrophytic input from the lower to the upper sections of the Raniganj Formation. This transition indicates probable progression of aquatic plants from submerged to an emergent type, indicating an environmental shift from the bottom to the top in the Raniganj Formation (Fig. 3).

The terrigenous to aquatic ratio, $(TAR) = (nC_{27}+nC_{29}+nC_{31})/(nC_{15}+nC_{17}+nC_{19})$, is commonly used to differentiate the source of organic matter of terrestrial or marine origin. Higher values (> 1) for this metric suggest more lipid content from the watershed than from aquatic sources (Bourbonniere & Meyers, 1996), and a lower value (< 1) indicates an aquatic input. The studied Raniganj area samples with a TAR value < 1 suggest a significant aquatic contribution to this area (Fig. 3). Although the TAR ratio suggests prominent aquatic contribution, a stratigraphic shift in the OM supply can be marked from aquatic toward terrestrial regime (Fig. 3). Terrestrial marine discriminant $TMD = (nC_{25}+nC_{27}+nC_{29}+nC_{31}+nC_{33})/(nC_{15}+nC_{17}+nC_{19}+nC_{21}+nC_{23})$ is another ratio used to determine the terrestrial or marine source. Values > 1 suggest a substantial terrestrial matter input, whereas values < 0.5 indicate a high marine/aquatic input (Chairi, 2018). The Raniganj shale samples, with a TMD ratio between 0.2 and 0.6 (Table 3), reveal a substantial aquatic contribution. Both the TAR and TMD ratio of < 1 suggest a strong aquatic input to the area, along with an environmental shift in the OM supply from aquatic toward terrestrial source (Fig. 3).

The ratio of low molecular weight hydrocarbon (LMWH) to high molecular weight hydrocarbon (HMWH) is represented by:

$$\frac{(nC14+nC15+nC16+nC17+nC18+nC19+nC20)}{(nC21+nC22+nC23+nC24+nC25+nC26+nC27+nC28+nC29+nC30+nC31+nC32+nC33+nC34)}$$

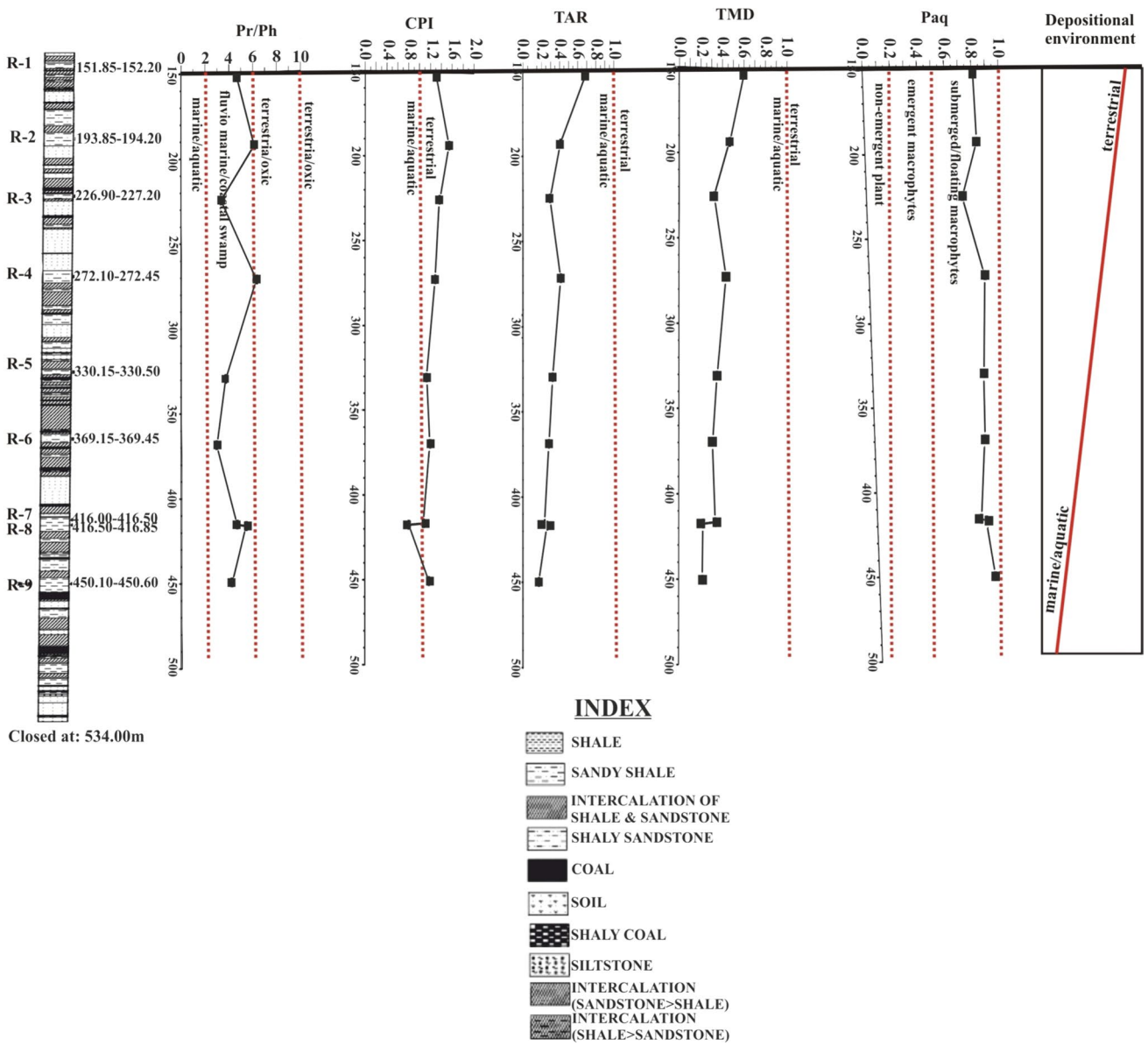

Fig. 3 Variation of *n*-alkane ratios with depth in Raniganj shales from Damoday Valley Basin

It assists in determining the source of organic matter from terrestrial to aquatic. An LMWH/HMWH ratio of < 1 indicates the OM input from higher terrestrial plants, sedimentary bacteria, and marine animals, whereas a ratio of 1 or > 1 indicates an aquatic input (Gearing et al., 1976; Kanzari et al., 2012; Wang et al., 2006). Here, the examined samples with an LMWH/HMWH ratio > 1 suggest organic-matter input mostly from aquatic sources.

4.2 Terpanes

Hopane (*m*/*z* 191) isomers have a consistent abundance in the range of nC_{27} to nC_{34}, with C_{30} 17αH,21βH hopane being the most abundant (Fig. 5). A decreased C_{29}/C_{30} hopane ratio indicates a suboxic to oxic environment. In high-sulfur oils, certain characteristics are commonly observed, such as a low-Pr/Ph ratio, diminished diasterane levels, elevated C_{35} homohopanes, and an increased C_{29}/C_{30} hopanes ratio. These features collectively suggest an anoxic depositional environment. Similarly, a high C_{29}/C_{30} ratio (> 1) implies a marine carbonate source rock, whereas a low ratio (< 1) indicates a marine shale to deltaic shale source rock (Peters et al., 2005). A C_{29}/C_{30} hopane ratio below 1 in the examined samples suggests that the source rock is predominantly composed of marine/deltaic shale.

C_{20}–C_{21}–C_{23} tricylicterpanes (TTs) can be used as a robust tool to identify the paleo-depositional environment (Wang et al., 2023). The relative prevalence of C_{20}–C_{21}–C_{23}

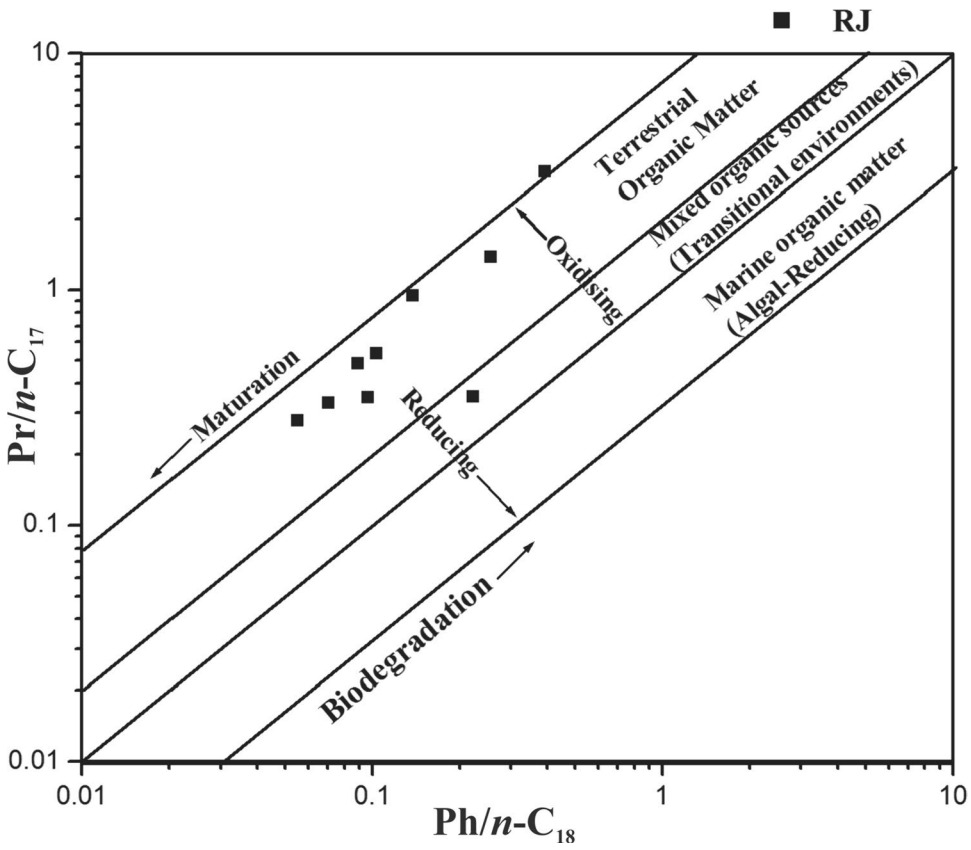

Fig. 4 Cross plot between Pr/C_{17} and Ph/C_{18} ratios indicating the kerogen type and thermal maturity of shales from the Damodar Valley basin (modified after Peter et al., 2005)

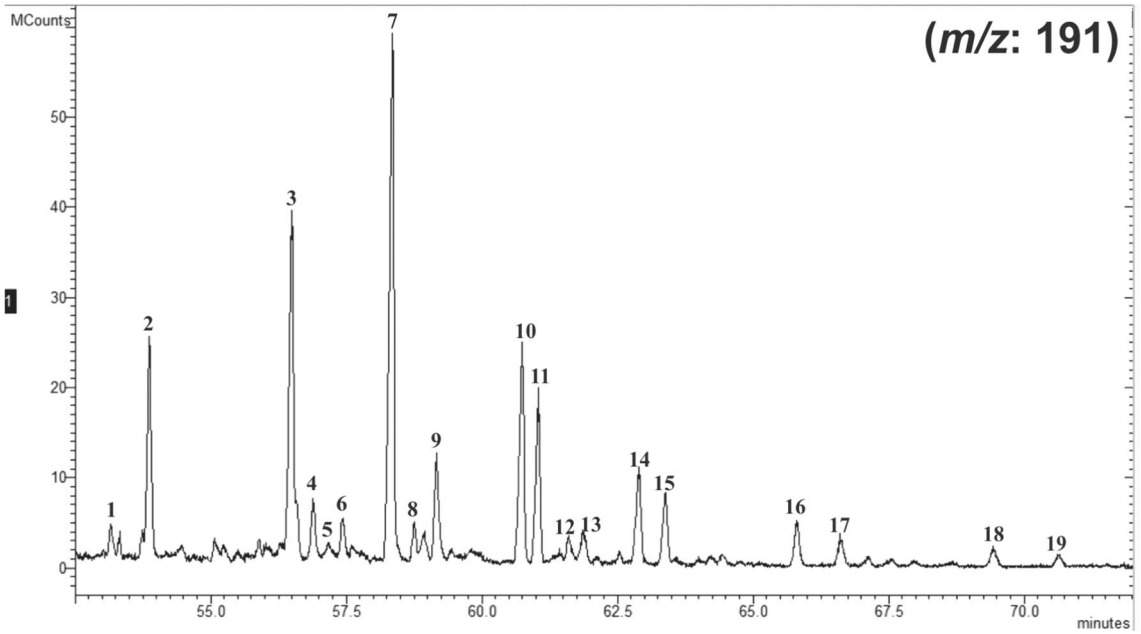

Fig. 5 Representative hopanes (*m/z* 191) distribution in sample R-4, 1 = C_{27} 18αH-trisnorhopane (Ts), 2 = C_{27} 17αH-trisnorhopane (Tm), 3 = C_{29} 17αH,21βH 25-norhopane, 4 = C_{29} 18αH-neohopane (29Ts), 5 = C_{30} 17αH diahopane, 6 = C_{29} 17βH,21αH-normoretane, 7 = C_{30} 17αH,21βH-hopane, 8 = C_{30} 30-Nor-29-homo-17αH-hopane, 9 = C_{30} 17βH,21αH-moretane, 10 = C_{31} 17αH,21βH-homohopane (22S), 11 = C_{31} 17αH,21βH-homohopane (22R), 12 = homohop-30-ene, 13 = C31 17βH-21βH-homohopane, 14 = C_{32} 17αH,21βH-bishomohopane (22S), 15 = C_{32} 17αH,21βH-bishomohopane (22S), 16 = C_{33} 17αH,21βH-trishomohopane (22S), 17 = C_{33} 17αH,21βH-trishomohopane (22R), 18 = C_{34} 17αH, 21βH-tetrahomohopane (22S), 19 = C_{34} 17αH,21βH-tetrahomohopane (22R)

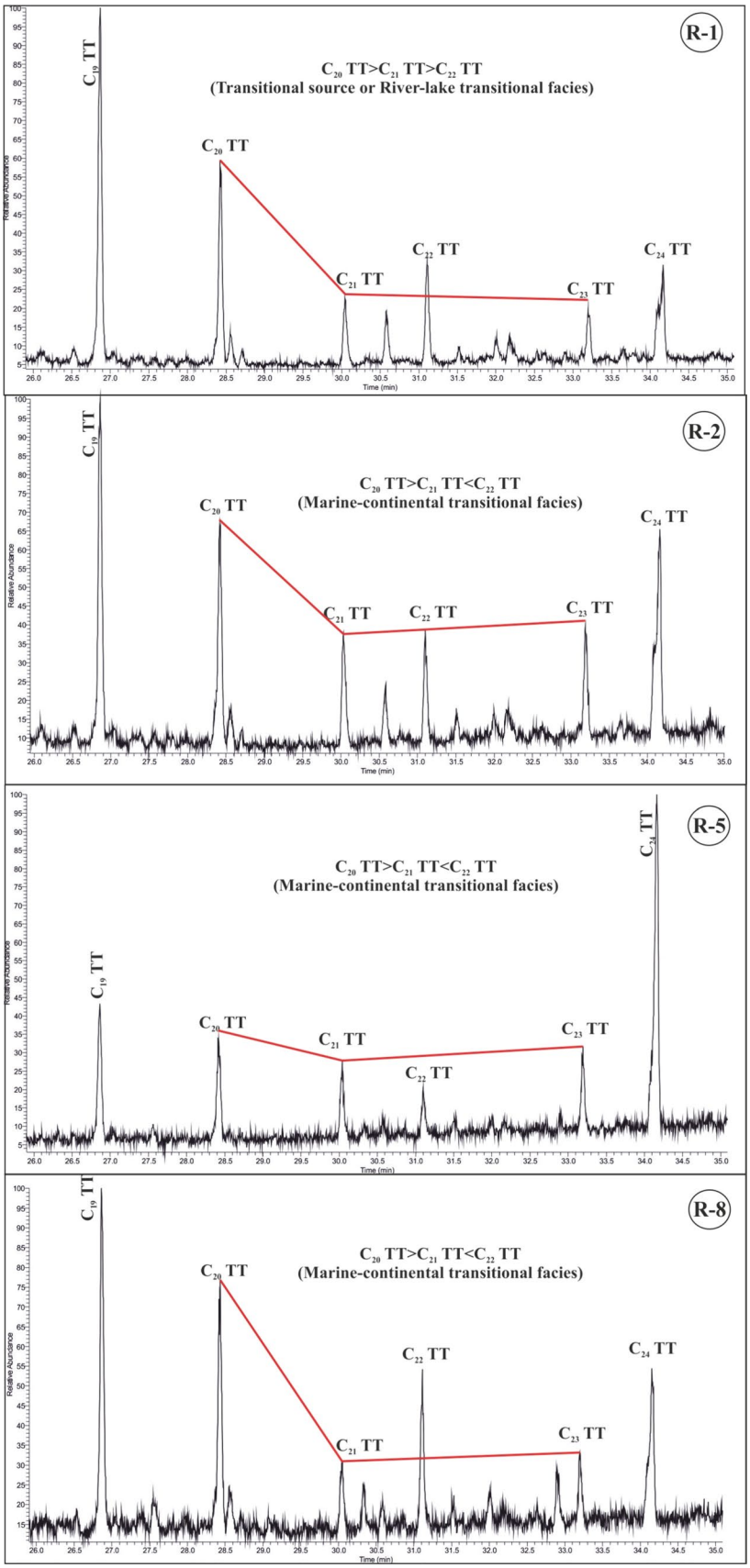

Fig. 6 Abundance pattern of C_{20}–C_{21}–C_{23} tricyclic terpanes deciphering different depositional settings

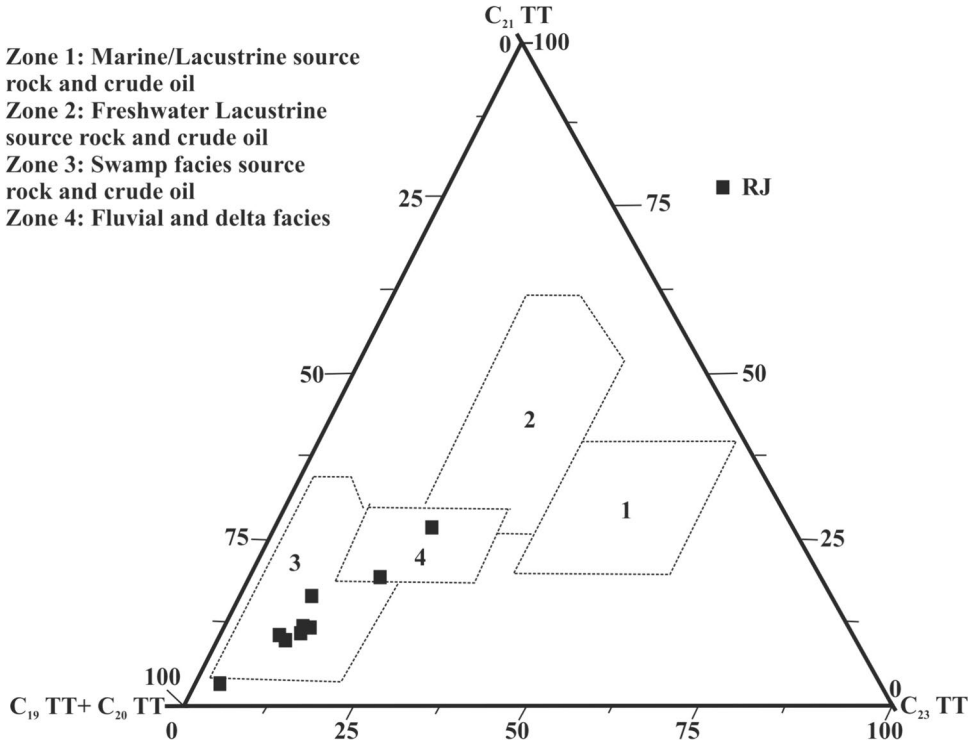

Fig. 7 Ternary diagram of TTs showing depositional environment for Raniganj shales (modified after Amoako et al., 2024)

TTs in sedimentary rocks and oils is influenced by the proportional input from planktonic organisms and terrestrial vegetation. Although the precise origins of TTs remain elusive (Dutta et al., 2006; Philp et al., 2021), several researchers have highlighted a strong correlation between TTs and depositional settings (Wang et al., 2023). C_{23} TTs frequently emerge as the predominant homolog in marine facies (Tao et al., 2015), while freshwater lacustrine environments commonly exhibit a prevalence of C_{21} TTs (Wang et al., 2023). In addition, terrestrial oils typically showcase heightened levels of C_{19} and C_{20} TTs (Peters & Moldowan, 1993). Distinctive patterns in the abundance of C_{20}–C_{21}–C_{23} TTs are observed across various depositional environments, encompassing marine and saline lacustrine, freshwater lacustrine, shallow-water terrestrial, and marine-continental transitional facies. These environments manifest unique compositions, with clear delineations observed among them. In marine and saline lacustrine facies, the abundance hierarchy follows $C_{20} < C_{21} < C_{23}$ TT, indicating a prevalence of C_{23} TT. Conversely, freshwater lacustrine facies exhibit a contrasting pattern, with $C_{20} < C_{21} > C_{23}$ TT. Shallow-water terrestrial facies demonstrate an abundance hierarchy of $C_{20} > C_{21} > C_{23}$ TT, suggesting a higher prevalence of C_{20} TTs. In marine-continental transitional facies, the hierarchy shifts again, with $C_{20} > C_{21} < C_{23}$ TT, being the prevailing pattern (Wang et al., 2023). These distinct abundance patterns serve as valuable indicators of the specific depositional conditions and environmental characteristics associated with each facies. The examined Raniganj shales show a transition in depositional environment from marine-continental transitional facies to transitional source/river–lake transitional facies (Fig. 6). This transition is observed from the lower to upper strata, indicating a shift from aquatic to terrestrial conditions consistent with the earlier findings regarding *n*-alkanes and isoprenoids. The ternary diagram further indicates a shift in the depositional environment between zone 3 to zone 4, reflecting a shift from swampy facies to fluvial delta facies (Fig. 7).

Further, the C_{23}/C_{21} and C_{21}/C_{20} TT ratios offer insights into paleo-depositional conditions, as well as past salinity and water depth levels. The ratio of C_{23}/C_{21} TT tends to increase with higher salinity levels in the depositional water, while the ratio of C_{21}/C_{20} TT shows a corresponding rise with greater depth of the depositional water column (Wang et al., 2023). The cross-plot between C_{23}/C_{21} and C_{21}/C_{20} indicates a shift in the depositional environment from marine-continental transitional to river–lake transitional (Table 3; Fig. 8).

Terpanes also offer insights into the temperature history and thermal maturity of source rocks. Seifert and Moldowan (1978) reported that C_{27} 17αH-trisnorhopane (Tm or 17α-22,29,30-trisnorhopane) is less stable during catagenesis than C_{27} 18α-trisnorhopane II (Ts or 18α-22,29,30-trisnorhopane). Hong et al. (1986) observed consistent increase in the relative abundance of Ts and an abrupt reduction in Tm value with depth. At the maturity comparable to the earliest oil window, Tm concentration approaches zero (Peters et al., 2005). Therefore, the Ts/(Ts + Tm), commonly

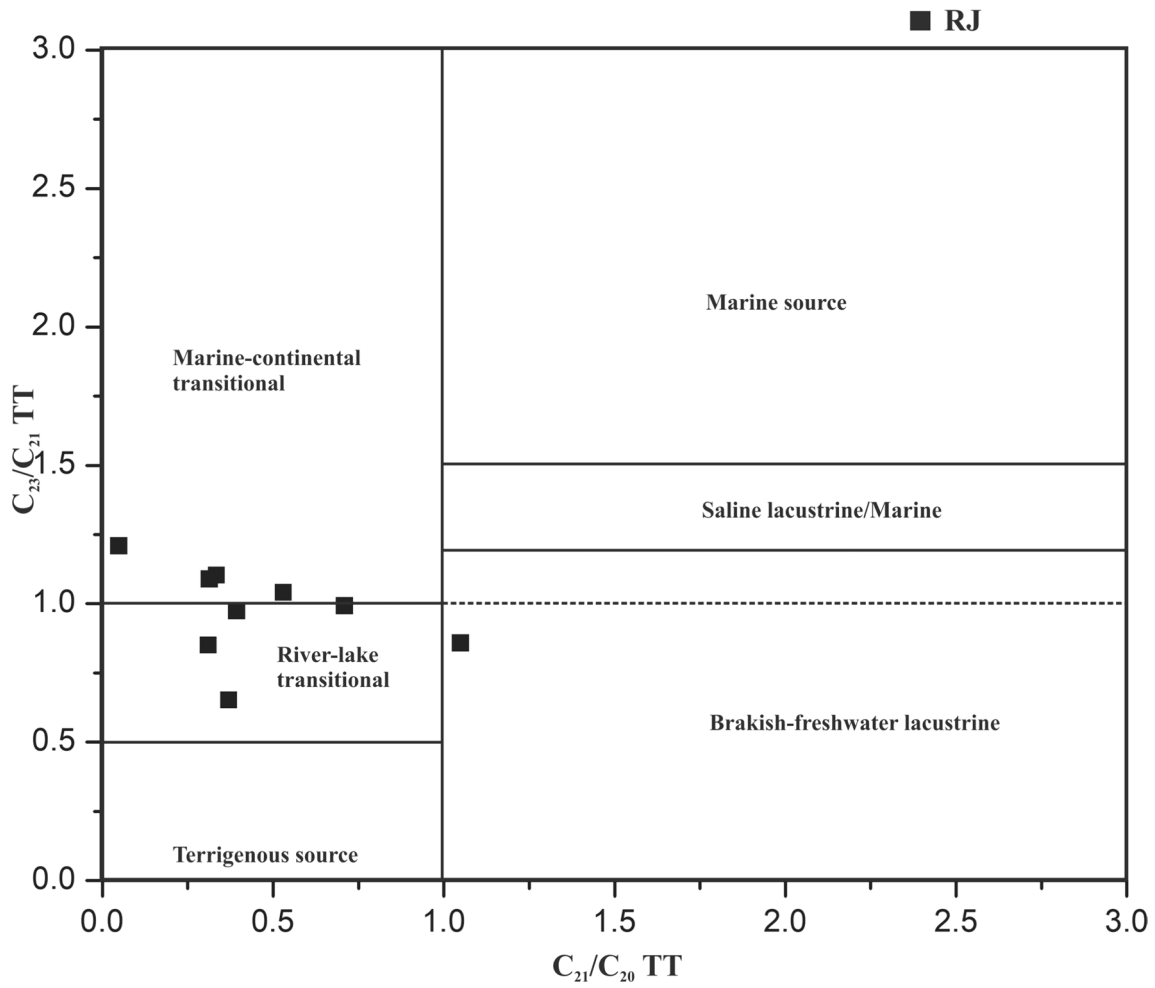

Fig. 8 C_{23}/C_{21} TT vs. C_{21}/C_{20} TT to decipher the paleo-depositional conditions in Raniganj shales

referred to as Ts/Tm, which is influenced by both the source of organic-matter input and maturity, can be utilized to determine the thermal maturity of source rocks. The Ts/(Ts + Tm) ratio in the Raniganj samples is < 1, indicating that the samples contain less stable Tm (C_{27} 17H-trisnorhopane). However, an increase in the Ts/(Ts + Tm) ratio with depth is accompanied with a decrease in the concentration of less stable Tm (C_{27} 17H-trisnorhopane) and an increase in the maturity of the examined samples with depth (Table 3; Fig. 9).

In addition, C_{30} 17αH diahopane (C_{30} D) and C_{29} 18αH-neohopane (C_{29} Ts) are identified as rearranged structures exhibiting elevated thermal stability, thus rendering them pertinent candidates for inclusion in thermal maturity study. The 17α-diahopane series (C_{30} D) demonstrates greater stability compared to the 18α-neohopane series (C_{29} Ts), with the latter exhibiting higher stability than the 17α-hopane series (C_{27} Ts) (Moldowan et al., 1991; Zhang et al., 2022). Consequently, the progression of maturity is expected to lead to heightened ratios of C_{30} D/C_{29} Ts. The examined sample shows a constant increase in the C_{30} D/C_{29} Ts ratio with depth (Table 3; Fig. 9).

C_{31} 22S/(22S + 22R) is another thermal maturity indicator that equilibrates at 0.57–0.62 and is used to determine whether samples are immature, in the oil window, or over mature. Samples with a 22S/(22S + 22R) ratio 0.50–0.54 indicate an early oil-window stage, whereas a ratio of 0.57–0.62 indicate peak oil-generation stage (Peters et al., 2005). The 22S/(22S + 22R) ratio of the examined samples vary between 0.53 and 0.93 (average ~ 0.62) indicating peak oil-generation stage has reached (Table 3; Fig. 9).

4.3 Steranes

Steranes (*m*/*z* = 217) have peaks in the nC_{27}–nC_{29} range with highest peak of C_{29}αββ sterane (20R) (Fig. 10). Relative abundance of C_{27}, C_{28}, and C_{29} sterane homologs can be used to decipher the paleo-vegetation input and depositional environment. Elevated concentrations of C_{29} sterane imply

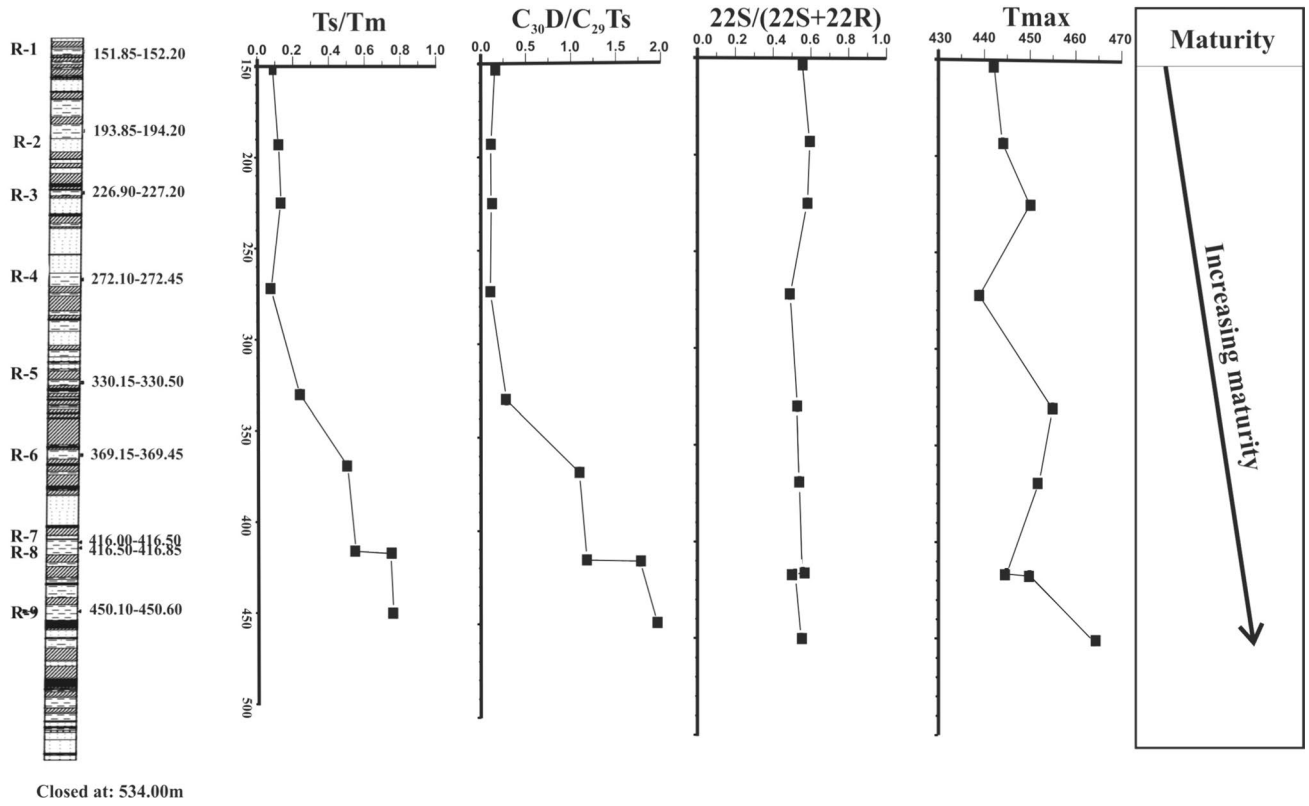

Fig. 9 Thermal maturity parameters indicating increasing maturity with depth (T_{max} is adopted form Mani et al., 2015; for lithology refer Fig. 3)

enhanced contributions from terrestrial plant sources, while increased levels of C_{27} sterane suggest the prevalence of algal input within a marine lacustrine to estuarine setting (Peters et al., 2005). The Raniganj shales, with an abundance of C_{29} sterane, mark dominant inputs from higher terrestrial plants, with subordinate supply from aquatic sources (Table 3; Fig. 11).

The thermal maturity in C_{29}20S/(20S + 20R) isomers continuously increase between 0.1 and 0.5 (with equilibrium between 0.52 and 0.55) (Seifert & Moldowan, 1986). As organic-matter ages, changes occur in the isomerization at positions C_{14} and C_{17} within the C_{29} 20S and 20R regular steranes. This process leads to an increase in the ββ/(αα + ββ) ratio, transitioning from values close to zero to approximately 0.7 (with equilibrium ranging from 0.67 to 0.71) (Seifert & Moldowan, 1986). Importantly, this ratio is not influenced by the source organic-matter intake and tends to take a bit longer to reach equilibrium compared to the 20S/(20S + 20R) ratio. Consequently, it proves to be a more valuable indicator, particularly at higher degrees of maturity (Peters et al., 2005). Majority of the examined samples of the Raniganj Formation are at equilibrium to post-equilibrium stage, suggesting the samples have reached peak oil-window stage (Fig. 12).

4.4 Aromatic hydrocarbons

The aromatic biomarkers in the Raniganj shales include the naphthalene, phenanthrene, biphenyl, and their alkylated derivatives, as well as a relatively lower abundance of dibenzothiophene and its analogs (Table 4). In the aromatic fractions of the shale extracts, alkylated homologues such as methyl naphthalenes (MN), ethyl naphthalenes (EN), dimethyl naphthalenes (DMN), trimethyl naphthalenes (TMN), and ethyl–methyl naphthalenes (EMN) were identified (Fig. 13). In addition, among the tricyclic aromatic hydrocarbons, phenanthrene (P), methyl phenanthrenes (MP), and various dimethyl phenanthrene isomers were also detected (Fig. 14). Phenanthrene and its derivatives are the dominant compounds present in the aromatic extract of the shales, followed by the naphthalene group (Table 4; Figs. 13, 14). The distribution of aromatic hydrocarbons and their alkyl derivatives is significantly influenced by the thermal maturation of organic matter. α-Substituted isomers of polynuclear aromatic systems are more sterically hindered and less thermodynamically stable compared to β-substituted isomers (Alexander et al., 1985; Garrigues et al., 1988; Simoneit & Fetzer, 1996). The α/β isomer ratios are known to be dependent on maturity, and these ratios were used in the calculation of temperature-sensitive maturity parameters like methyl

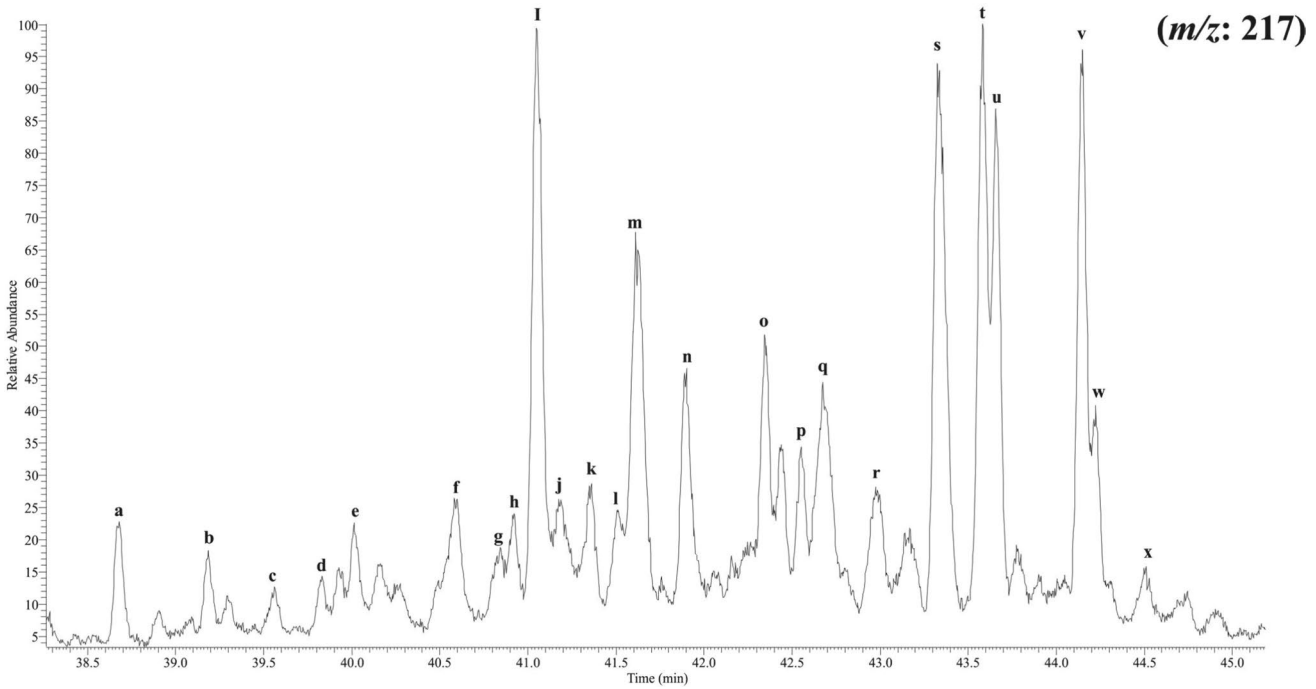

Fig. 10 Representative steranes (*m/z* 217) distribution in sample R-4, a = C_{27}βα diasterane (20S), b = C_{27}βα diasterane (20R), c = C_{27}αβ diasterane (20S), d = C_{27}αβ diasterane (20R), e = C_{28}βα diasterane (20S), f = C_{28}βα diasterane (20R), g = C_{28}αβ diasterane (20S), h = C_{27}ααα sterane (20S), i = C_{27}αββster-(20R) + C_{29}βαdia-(20S), j = C_{27}ααα sterane (22S), k = C_{28}αβ diasterane (20R), l = C_{27}ααα sterane (20R), m = C_{29}βα diasterane (20R), n = C_{27}αβ diasterane (20S), o = C_{28}ααα sterane (20S), p = C_{29}αβ diasterane (20R), q = C_{28}ααβ sterane (20R), r = C_{28}ααα sterane (20R), s = C_{29}ααα sterane (20S), t = C_{29}ααβ sterane (20R), u = C_{29}ααβ sterane (20S), v = C_{29}ααα sterane (20R), w = C_{30}ααα sterane (20S), x = C_{30}ααβ sterane (20R)

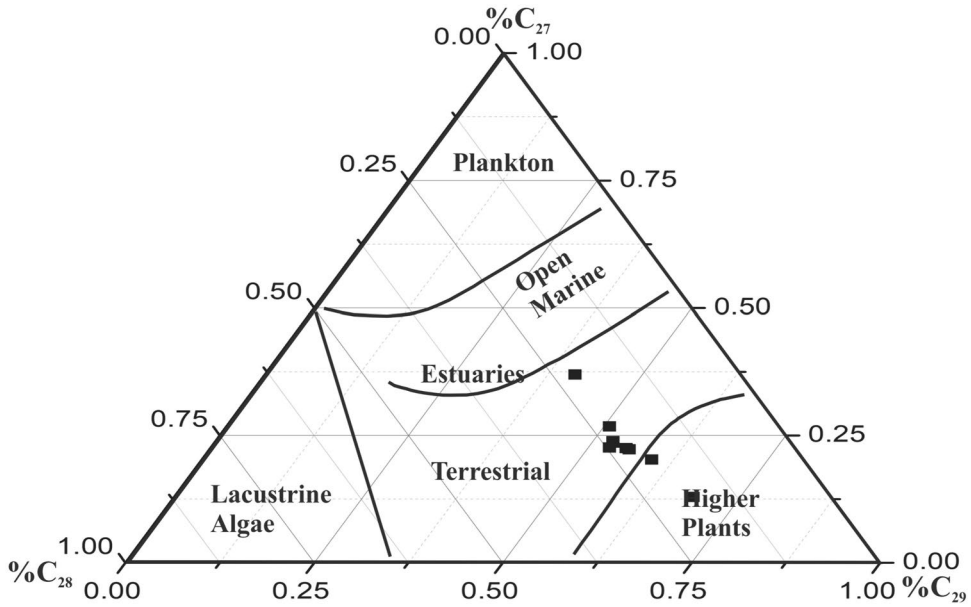

Fig. 11 C_{27}–C_{28}–C_{29} sterane ternary diagram depicting source of organic matter in Raniganj shales from Damodar Valley Basin

phenanthrene indices (MPI-1), dimethyl naphthalene ratios (DNR-1 and DNR-2), and trimethyl naphthalene ratio (TNR-1) (Table 4). The ratios observed in the Raniganj shales, in general, are high, which suggesting mature to highly mature state of organic matter (Table 4).

Aromatic compounds found in crude oils and ancient sediments are thought to originate from the thermal degradation

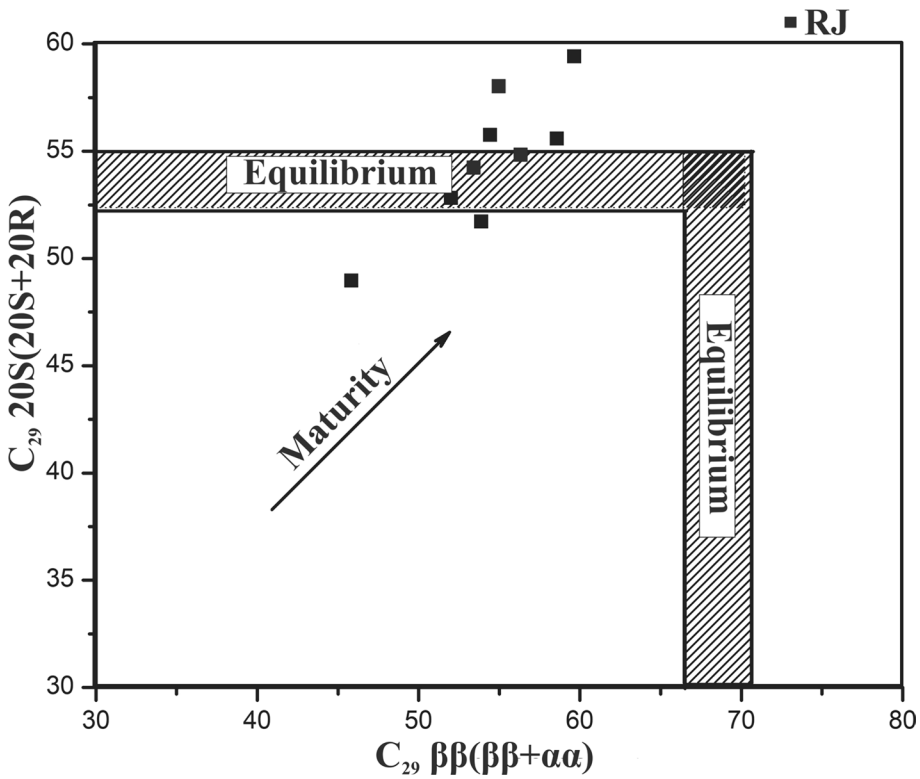

Fig.12 Cross-plot between C29 steranes in Raniganj Shales, Damodar Valley Basin (modified after Peters, 1999)

of biologically produced compounds, including steroids and terpenoids (Hall et al., 1985; Strachan et al., 1988). Steroids are believed to give rise to substituted phenanthrenes, while terpenoids are associated with the production of alkyl naphthalenes (Hall et al., 1985; Strachan et al., 1988). In addition, alkyl naphthalenes can potentially originate from the thermal degradation of spores, coals, and sporopollenin (Allan & Larter, 1981), as well as cyclic sesquiterpenoids found in resinous components (Peters et al., 2005). In the case of alkylated phenanthrenes, one major source appears to be terpenoids derived from higher plant constituents, such as resins and waxes (Tissot & Welte, 1984). The high amount of terrigenous plant material in the Raniganj shales is the precursor, which upon thermal cracking, followed by high-temperature rearrangements in the cyclic structure led to the formation of these aromatic molecules. Radke et al. (1982) proposed that the direct methylation of phenanthrene during the catagenesis process could be a significant source of alkyl phenanthrenes. In addition, the conversion of higher plant triterpenoids within sediments into aromatic hydrocarbons occurs through the removal of oxygen functional groups and subsequent ring aromatization (Johns, 1986; Radke, 1987; Rullkotter et al., 1994). The end products of these processes are tetracyclic and pentacyclic aromatic hydrocarbons. As diagenesis and catagenesis progress, these tetracyclic and pentacyclic aromatic hydrocarbons can undergo cleavage of bonds within their rings. This, coupled with photochemical and acid-catalyzed processes, leads to the formation of methyl-substituted naphthalenes and phenanthrenes, respectively (Radke, 1988; Radke et al., 1982; Seifert & Moldowan, 1978, 1986).

Compounds such as biphenyl, dibenzofuran, fluorene and their methylated homologues were observed in almost all the aromatic hydrocarbon fractions of the studied samples. These compounds are likely products of degradation of lignin during digenesis (Radke, 1988; Radke et al., 1982; Seifert & Moldowan, 1978, 1986). The presence of low dibenzothiophene/phenanthrene (DBT/P) ratios (ranging from 0.01 to 0.67), along with a higher concentration of 1,2,5-TMN compared to 1,2,7-TMN, strongly suggests that the organic matter is primarily derived from terrestrial plants. These two molecular indicators, the DBT/P ratio and the Pr/Ph ratio, can also serve as valuable tools for deducing the depositional environments and lithologies of source rocks (Hughes et al., 1995; Peters et al., 2005). The DBT/P ratio of the Permian shales from Raniganj Formation has been shown in (Fig. 15) which indicates a source material consists of fluvial-deltaic shale and coal. Radke et al. (1982) attempted to determine the thermal maturity of coals based on methylphenanthrene index (MPI-1) derived from the composition of compounds extractable from coals by organic solvents. It was given by:

$$\mathrm{MPI1} = 1.5(2 - \mathrm{MP} + 3 - \mathrm{MP})/P + 1 - \mathrm{MP} + 9 - \mathrm{MP},$$

Table 4 Aromatic biomarker concentrations (µg/gTOC) and ratios in the Raniganj shales from Jharia sub-basin, Damodar Valley

Compound	R-2	R-4	R-7	R-8
2-MN	29.1	9.7	2.3	38.6
1-MN	19.8	8.9	1.1	30.1
2-EN	3.7	2.5	0.3	4.5
1-EN	2.1	2.4	4.1	2.0
2,6-+2,7-DMN	13.7	15.4	4.1	39.1
1,3+1,7-DMN	16.8	20.5	5.7	50.6
1,6-DMN	15.1	17.3	5.0	44.6
1,4+2,3-DMN	7.7	9.8	2.4	20.2
1,5-DMN	4.3	5.2	1.2	11.8
1,2-DMN	8.2	8.0	1.9	13.5
PrN+EMN	1.4	26.4	0.8	0.6
PrN+EMN	3.9	30.6	0.1	0.6
PrN+EMN	6.4	14.3	0.3	6.2
PrN+EMN	1.1	1.6	0.5	3.5
1,3,7-TMN	3.4	6.9	2.9	16.0
1,3,6-TMN	6.4	13.1	4.4	22.3
1,3,5-+1,4,6-TMN	7.8	15.6	3.5	20.1
2,3,6- TMN	4.2	9.7	3.0	14.3
1,2,7-+1,6,7-+1,2,6-TMN	7.6	14.4	4.6	23.5
1,2,7-+1,6,7-+1,2,6-TMN	7.2	10.3	3.8	17.8
1,2,5-TMN	31.1	37.6	5.7	27.8
DBT	19.2	5.4	3.9	7.6
P	28.8	36.4	23.6	89.0
MDBT	0.3	0.4	0.1	5.2
3-MP	9.4	15.9	11.3	42.7
2-MP	9.5	16.9	12.0	44.2
9-MP	14.5	17.8	16.7	66.2
1-MP	10.8	15.2	12.7	51.0
9-+1-EP+3,6-DMP	2.9	6.2	2.4	9.5
3,5-+2,6-DMP	1.0	5.5	0.7	9.5
2,7-DMP	2.1	7.1	2.4	7.6
1,3-+3,9-+2,10-+3,10-DMP	2.1	15.9	2.0	54.0
1,6-+2,9-+2,5-DMP	7.9	12.3	12.9	30.0
1,7-DMP	5.8	10.7	7.4	28.3
2,3-+1,9-DMP	6.0	3.7	6.9	7.6
4,9-+4,10-DMP	2.0	3.3	2.2	12.7
1,8-DMP	1.7	4.3	2.8	6.3
1,2-DMP	1.5	3.3	1.4	9.7
Ratios				
DNR-1	3.2	3.0	3.4	3.3
DNR-2	1.8	1.6	1.7	1.9
MPI-1	0.5	0.7	0.7	0.6
TNR-1	0.5	0.6	0.8	0.7
DBT/P	0.7	0.2	0.2	0.1

MN methyl naphthalene, *EN* ethyl naphthalene, *DMN* dimethyl naphthalene, *TMN* trimethyl naphthalene, *PrN* propyl naphthalene, *EMN* ethyl–methyl naphthalene, *DBT* dibenzothophene, *P* phenanthrene, *MDBT* methyl dibenzothiophene, *MP* methyl phenanthrene, *DMP* dimethyl phenanthrene

where *P* is phenanthrene, 2-MP is 2-methylphenanthrene, 3-MP is 3-methylphenanthrene, 1-MP is 1-methylphenanthrene, and 9-MP is 9-methylphenanthrene.The methylphenanthrene ratio (MPI-1) revealed a linear correlation with the measured vitrinite reflectance (Ro%) of the coals (Radke et al., 1982, 1987). The MPI-1 and mean Ro% correlations of samples from Raniganj Formations show that these samples are in oil-generation stage (Fig. 16).

4.5 Late Permian Gondwana surface environments

The effectiveness of biomarkers as indicators of depositional environments stems from the fact that these naturally occurring molecular fossil compounds are linked to specific communities of organisms or plants that thrive in particular habitat conditions, while their preserved record represents depositional regime in which the sedimentary rocks get deposited. The Upper Permian Raniganj Formation overlies the other Gondwanan Formations of Barren Measures and Barakar in Jharia Sub-basin. The lithology of these formations are marked by coarse to fine-grained sandstones, shales, carbonaceous shales and coal seams. The evidence from paleocurrent patterns, channel morphology, texture, and petrography strongly indicates that the sedimentation of the Raniganj Formation occurred within a vast and cohesive alluvial plain (Cassyap & Kumar, 1987; Cassyap & Tewari, 1987). In the Jharia and Raniganj coalfields, while clear marine characteristics have not been conclusively identified, the elevated levels of boron, vanadium, and chromium, along with the presence of *skolithos* and *thalassinoid* burrows, do raise the possibility of a brackish water environment (Gupta, 1999). According to Ghosh (2003), during Permian Period, the Damodar Basin was located within the extended marine embayment region, characterized by interactions with the Tethys sea. Similarly, reports from Gupta (1991, 1992) in the Ramgarh coalfield, Mukhopadhyay (1996) in the South Karanpura and West Bokaro coalfields, and Chandra (1992) in the Jharia coalfield have suggested the possibility of marine influences or incursions in the basin. According to Gupta (1999), the upper part of the sedimentary record indicates that these sediments were likely deposited in a geographic location very close to the sea or at the sea's edge, possibly within a peri-tidal setting. Storm activity played a significant role during this sedimentation process, indicating the presence of a broad and shallow sea, often referred to as an epeiric or epicontinental sea, which developed during periods of elevated sea levels (Gupta, 1999).

The biomarker distribution pattern in the Raniganj shales corroborate the geologic records in terms of the paleo-vegetation and depositional settings that prevailed during the

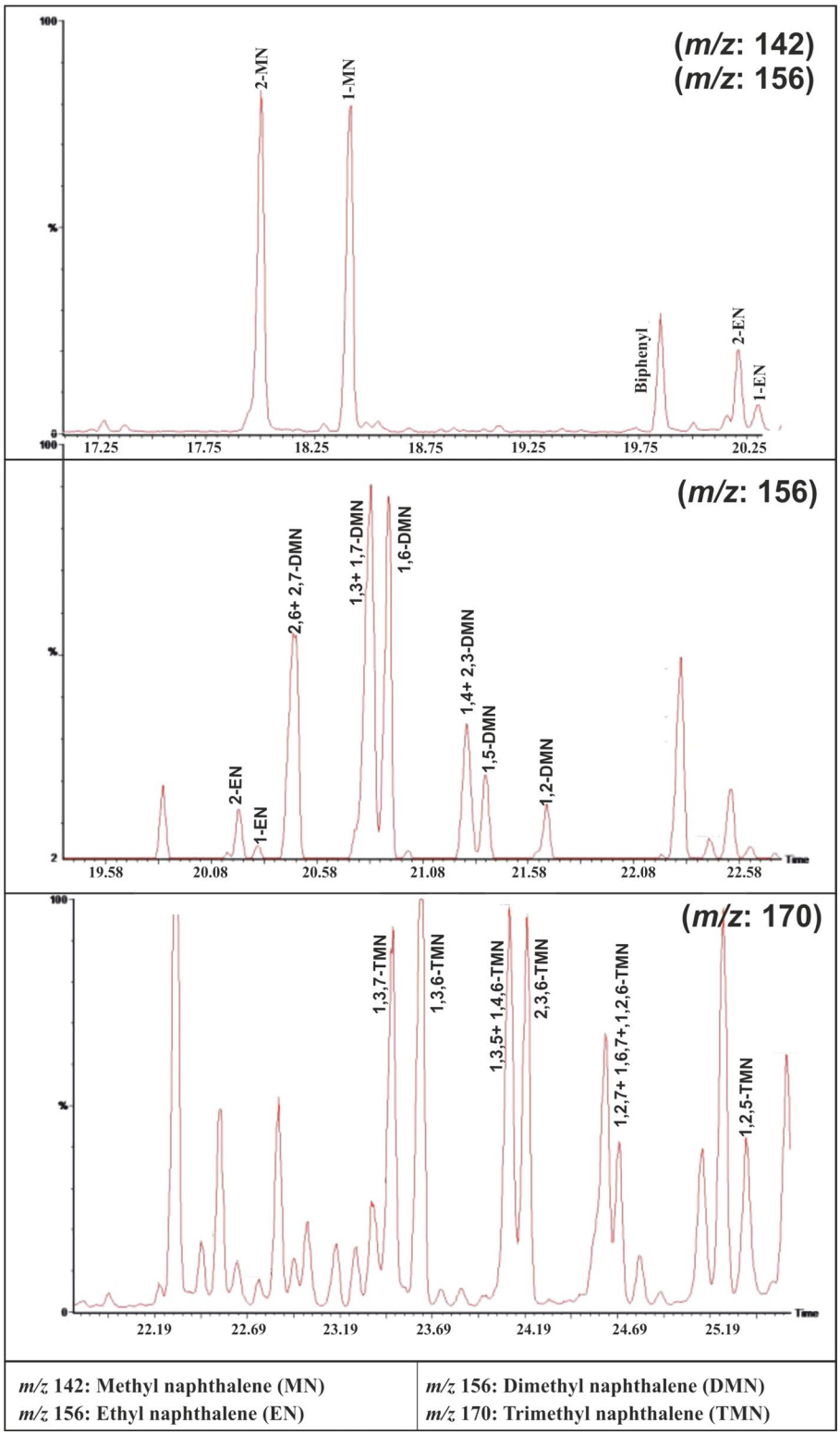

Fig. 13 Representative spectra of Aromatic biomarkers from sample R-4 (Naphthalene and its alkylated homologs) in the extracted organic matter of the shales from Raniganj Formation, Damodar Valley basin

Late Permian Period in Gondwanaland. The unimodal distribution of *n*-alkanes, peak around nC_{17}-Pristane, characterized by organic inputs mainly from aquatic algae, accompanied by increased microbial activities, whereas the CPI value varying between 0.82 and 1.55 marking the organic-matter input from aquatic and terrestrial sources (Fig. 3). Pr/Ph ratio in the range between 2 and 6 suggests organic-matter preservation within fluvial, swampy depositional environment (Fig. 3). Also, the Pr/n-C_{17} ratios ranging ≤ 1.0 indicate the swampy to open water conditions. The Pr/n-C_{17} and

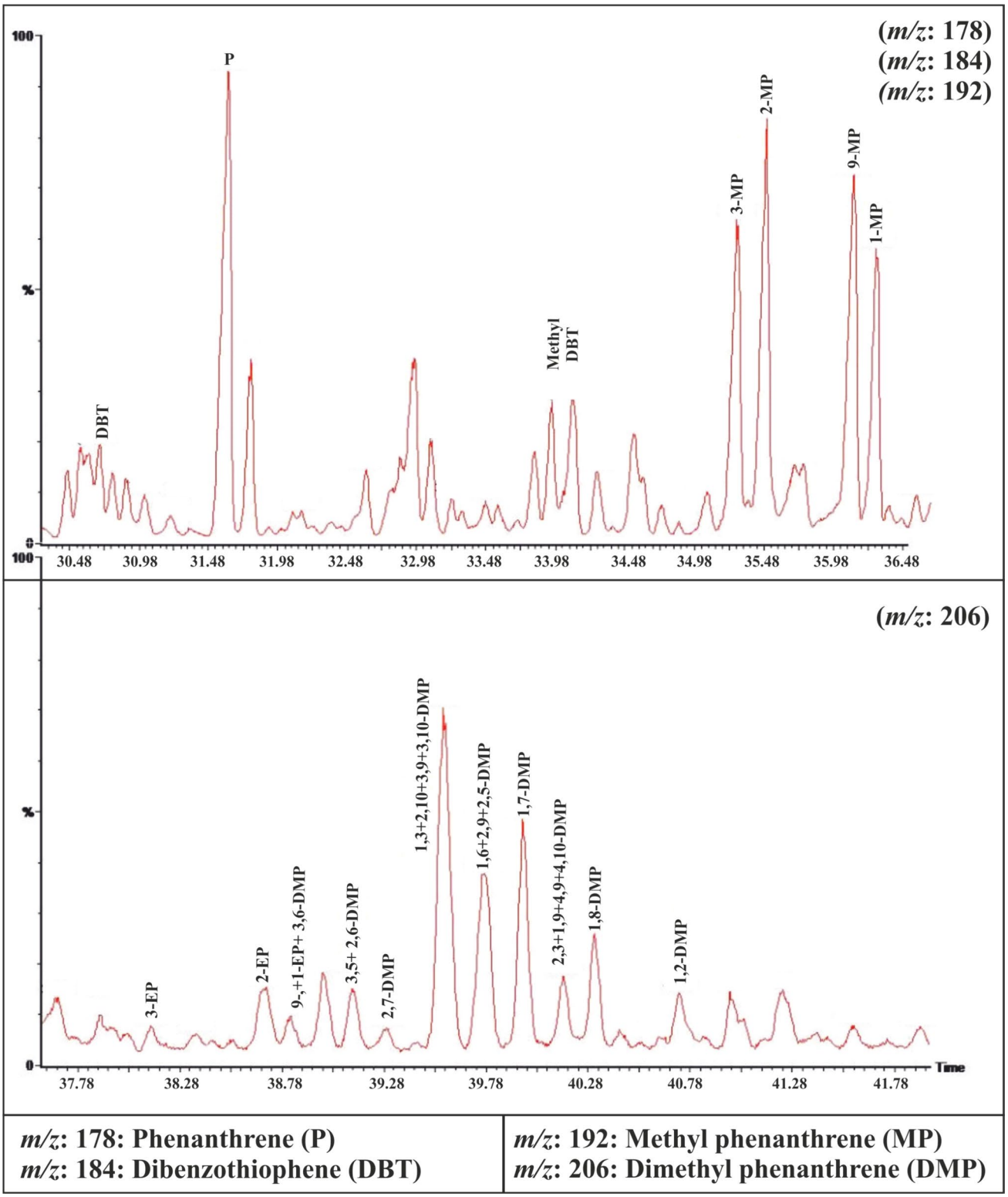

Fig. 14 Representative spectra of aromatic biomarkers from sample R-4 (Phenanthrene and its alkylated homologs) in the extracted organic matter of the shales from Raniganj Formation, Damodar Valley basin

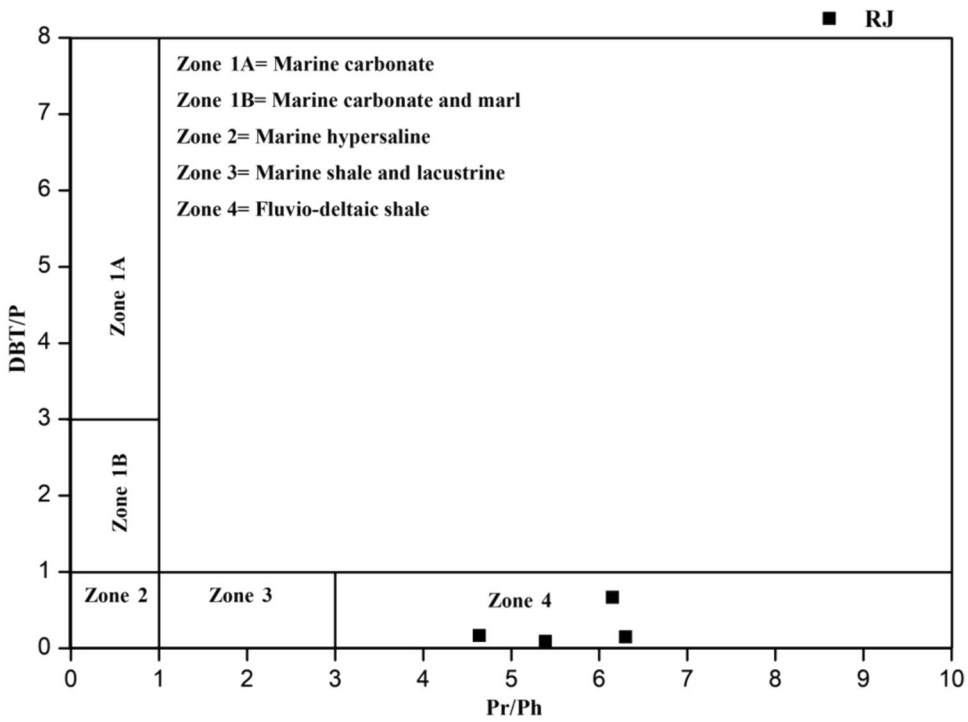

Fig. 15 Cross plot between Pr/Ph and DBT/P plot to show the depositional environment of shales from the Damodar Valley basin

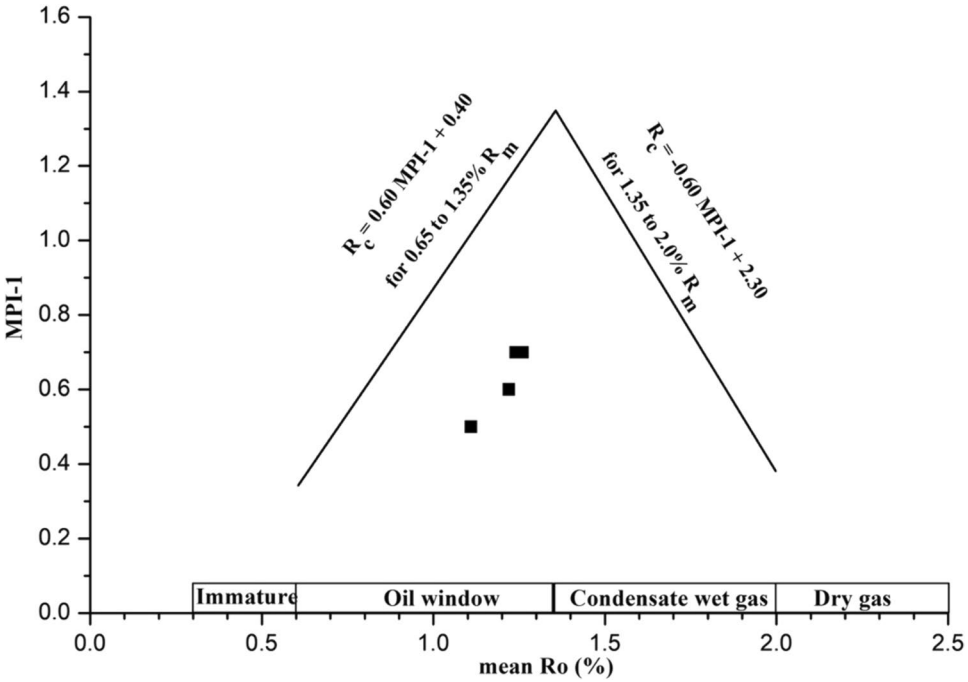

Fig. 16 Cross plot between Methyl Phenanthrene Index (MPI-1) and vitrinite reflectance indicating the maturity of shales from the Damodar Valley Basin

Ph/*n*-C_{18} correlations show an oxic, mixed Type-III kerogen input (Fig. 4). The Pr/Ph and DBT/P correlations diagram indicate the sample to lie in Zone 4, which represents a fluvial-deltaic shale and coal depositional setting (Fig. 15).

From the Proxy Ratio (P_{aq} = 0.7–0.8) the organic matter has been identified as submerged/floating macrophytes type (Fig. 3).This value is corroborated by the lower TAR and TMD ratio (< 1), which suggests a dominant signature of aquatic input (Fig. 3). Also, the elevated ratio of LMWH

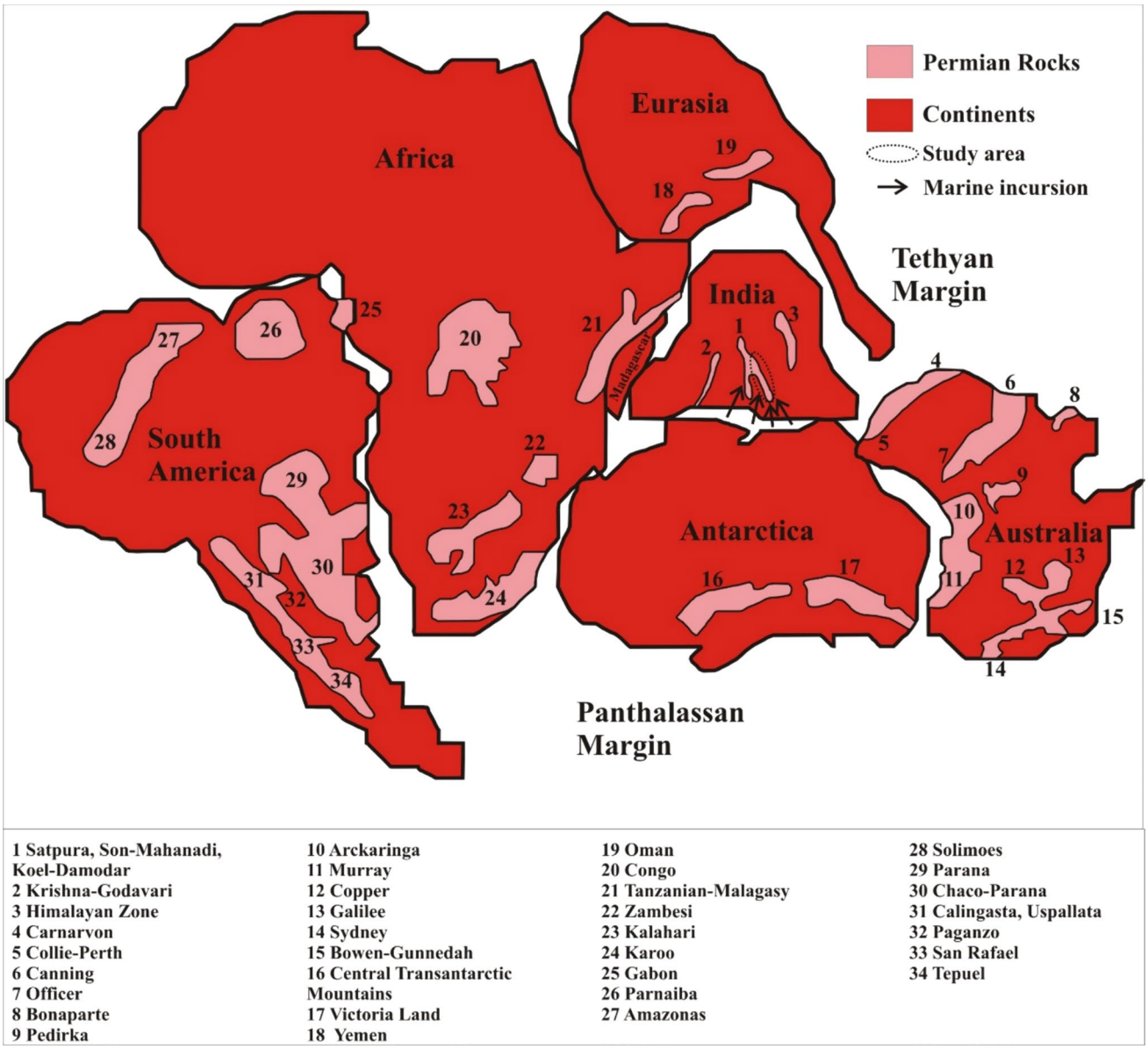

Fig. 17 Distinct basins in the Early Permian Gondwana Period. A possible marine-incursion activity to the Damodar basin from the paleo-Tethys Sea is marked by the arrows (modified after Stephenson et al., 2007)

to HMWH for the Raniganj shale represents an aquatic contribution to the organic matter. The variations in CPI, TAR, TMD, Paq ratios show a clear environmental shift in the depositional conditions from marine/aquatic toward terrestrial (Fig. 3). Similarly, the relative abundance of C_{20}–C_{21}–C_{23} TTs suggest a stratigraphic shift in the depositional environment from marine-continental transitional to transitional source/river–lake transitional facies (Fig. 6). In addition to assessing the relative abundance of TTs, the ternary diagram depicting $C_{19}+C_{20}$ TTs, C_{21} TTs, and C_{23} TTs illustrate a distinct shift in the depositional environment, transitioning from swampy facies to fluvial delta facies (Fig. 7). Similarly, the cross-plot of C_{23}/C_{21} against C_{21}/C_{20} delineate the transition from marine-continental transitional to river–lake transitional environments (Fig. 7). Overall, there is a gradational distribution of OM input, both from terrestrial and aquatic sources, indicating a noticeable shift in the depositional environment from marine/aquatic to terrestrial for this area (Fig. 3). This change in the depositional environment from marine/aquatic to terrestrial recorded in a stratigraphic manner and is reflection by the biomarker variability with depth in the Raniganj Formation. While the bottom samples are noted to be prone toward a marine/aquatic setting, the top samples gradually shift to terrestrial

environment (Figs. 3, 6). Below the coal-bearing Raniganj Formation, lies the Barren Measures, which deposited in lacustrine/near marine environment (Chandra, 1992; Mani et al., 2015). The biomarker proxies suggest a shift in the lacustrine/marine prevailing region during the deposition of the Barren Measures Formation to a terrestrial one for Raniganj Formation (Table 1). The Gondwana sequences are dominantly fluvial; however, there also exists the likeliness of partial marine ingression (Veevers & Tewari, 1995) and the suitability of the basin location for a marine-incursion activity from the paleo-Tethys Sea during the Gondwana time is shown in Fig. 17.

Various thermal maturity indicators for terpanes, such as Ts/Tm, C_{30} D/C_{29} Ts, and C_{31} 22S/(22S + 22R) ratios indicated a consistent progression toward higher thermal maturity with increasing depth (Fig. 9).The plot between MPI-1 and mean Ro% suggests the samples to be in the oil-generation stage of the maturity curve (Fig. 16). Globally, the Permian basins show evidence of oil and gas production and in recent times, these have attained yet another renaissance due to unconventional shale resource systems for gas (Jarvie et al., 2007; Murphy et al., 1972). Thermally matured, high organic-matter-rich shales with Type-III kerogen from Raniganj Formation suggest it to be a good gas generation prospect. However, the maturity levels in oil-window zone of these shales indicate that samples have not reached enough thermal maturity to undergo the gas generation. On the other hand, the Barakar and Barren Measures shales of this area show a maturity at the wet-gas to dry-gas stage (Mani et al., 2015). With Raniganj being the upper most formation of the studied Lower Gondwana basin, a lesser burial depth could be one reason for the lower thermal maturity of these samples to reach the gas generation stage.

5 Conclusion

The *n*-alkane, isoprenoids, hopanes, steranes and aromatic biomarkers have been used to understand the depositional environment and source rock characteristics of the Raniganj shales from the Jharia sub-basin of the Damodar Valley. Their abundance and ratios provided useful insight about the depositional settings of the Raniganj Formation. The studied shales are organically rich and thermally mature in the oil-generation stage. The organic matter was mainly derived from the terrestrial environments (Type-III Kerogen), deposited in an open water or swampy environment. The *Paq*, TAR, TMD, and LMWH/HMWH ratios and their variability across the formation from bottom to top suggest an aquatic input to the area, with a shift in depositional environment from marine/aquatic to terrestrial. Likewise, the environmental shift from marine-continental transitional to transitional source/river–lake transitional facies is evident from the abundance and distribution pattern of C_{20}–C_{21}–C_{23} TTs. The ternary diagram and cross-plot illustrate distinct transitions in depositional environments from swampy facies to fluvial delta facies and from marine-continental transitional to river–lake transitional environments, respectively. The observed environmental shift occurs in a stratigraphic pattern, with the environment progressively transitioning from marine/aquatic to increasingly terrestrial. This implies a geographic position relatively near to the sea or at the edge of the sea, potentially in a peri-tidal environment where wave activity was important during sedimentation. The Ts/Tm, C_{30} D/C_{29} Ts, C_{31} 22S/(22S + 22R), andMPI-1 and mean Ro% graph suggest that the Raniganj shales have reached the maturity of the oil-window stage. There is a systematic increase in the thermal maturity of these samples with depth, however; the shales in studied part of basin have not been buried enough to reach the gas generation stage.

Acknowledgements The Oil Industry Development Board, New Delhi is acknowledged for the financial support toward establishment of laboratory facility at Council of Scientific and Industrial Research-National Geophysical Research Institute (CSIR-NGRI). The Officials of Central Mine Planning and Design Institute (CMPDI), Ranchi and Drs. D. J. Patil and M. S. Kalpana are thanked for extending their support during field visits and analytical work. The authors acknowledge the reviewers for the constructive comments in improvement of the manuscript. The Director, NGRI is thanked for permitting the publication of this work. This contribution forms part of the SHORE Project of NGRI under the 12th Five Year Scientific Program of CSIR.

Author contributions NRK wrote initial draft, analysis and interpretation DM formulation of research problem, supervision, analysis, method development, interpretation and editing EVSSKB supervision and resources.

Data availability The data will be made available on request.

Declarations

Conflict of interest The authors declare no competing interests.

References

Alexander, R. (1992). An oil-source correlation study using age specific plant-derived aromatic biomarkers. *Biological markers in sediments and petroleum* (pp. 201–221). Prentice-Hall.

Alexander, R., Cumbers, K. M., & Kagi, R. I. (1986). Alkylbiphenyls in ancient sediments and petroleums. *Organic Geochemistry, 10*(4–6), 841–845.

Alexander, R., Kagi, R. I., Rowland, S. J., Sheppard, P. N., & Chirila, T. V. (1985). The effects of thermal maturity on distributions of dimethylnaphthalenes and trimethylnaphthalenes in some ancient sediments and petroleums. *Geochimica Et Cosmochimica Acta, 49*(2), 385–395.

Allan, J., & Larter, S. R. (1981). Aromatic structures in coal maceral extracts and kerogens. *Advances in organic geochemistry* (pp. 534–545). Wiley Heyden.

Amoako, K., Zhong, N., Shi, S., Konan, N. F. D. S., Osei-Boakye, N. P., Foli, G., Appau, P. O., Fenyi, C., & Apesegah, E. (2024).

Organic geochemical heterogeneity of cretaceous mudrocks and reassessment of oil sources in the Tano Basin, Ghana. *Marine and Petroleum Geology, 162*, 106697.

Bourbonniere, R. A., & Meyers, P. A. (1996). Sedimentary geolipid records of historical changes in the watersheds and productivities of Lakes Ontario and Erie. *Limnology and Oceanography, 41*(2), 352–359.

Cashyap, S. M., & Tewari, R. C. (1987). Depositional model and tectonic evolution of Gondwana basins. *Journal of Palaeosciences, 36*, 59–66.

Casshyap, S. M. (1970). Sedimentary cycles and environment of deposition of the Barakar coal measures of Lower Gondwana, India. *Journal of Sedimentary Research, 40*(4), 1302–1317.

Casshyap, S. M., & Kumar, A. (1987). Fluvial architecture of the Upper Permian Raniganj coal measure in the Damodar basin, Eastern India. *Sedimentary Geology, 51*(3–4), 181–213.

Chairi, R. (2018). Biomarkers on sediments in a highly saline aquatic ecosystem: Case of the Moknine Continental Sebkha (Eastern Tunisia). *Journal of Coastal Zone Management, 21*(2), 463.

Chandra, D. (1992). *Jharia coalfield. Mineral resources of India* (Vol. 5, p. 149). Geological Society of India.

Dasgupta, P. (2005). Facies pattern of the middle Permian Barren Measures Formation, Jharia basin, India: The sedimentary response to basin tectonics. *Journal of Earth System Science, 114*, 287–302.

Didyk, B. M., Simoneit, B. R. T., Brassell, S. T., & Eglinton, G. (1978). Organic geochemical indicators of palaeoenvironmental conditions of sedimentation. *Nature, 272*(5650), 216–222.

Dutta, S., Greenwood, P. F., Brocke, R., Schaefer, R. G., & Mann, U. (2006). New insights into the relationship between Tasmanites and tricyclic terpenoids. *Organic Geochemistry, 37*(1), 117–127.

Energy Information Assessment/Advanced Resources International Incorporation. (2013). EIA/ARI world shale gas and shale oil resource assessment. In *24th Chapter on India/Pakistan*, pp. 1–42.

Ficken, K. J., Li, B., Swain, D. L., & Eglinton, G. (2000). An *n*-alkane proxy for the sedimentary input of submerged/floating freshwater aquatic macrophytes. *Organic Geochemistry, 31*(7–8), 745–749.

Garrigues, P., De Sury, R., Angelin, M. L., Bellocq, J., Oudin, J. L., & Ewald, M. (1988). Relation of the methylated aromatic hydrocarbon distribution pattern to the maturity of organic matter in ancient sediments from the Mahakam delta. *Geochimica Et Cosmochimica Acta, 52*(2), 375–384.

Gearing, P., Gearing, J. N., Lytle, T. F., & Lytle, J. S. (1976). Hydrocarbons in 60 northeast Gulf of Mexico shelf sediments: A preliminary survey. *Geochimica Et Cosmochimica Acta, 40*(9), 1005–1017.

George, S. C., Lisk, M., Summons, R. E., & Quezada, R. A. (1998). Constraining the oil charge history of the South Pepper oilfield from the analysis of oil-bearing fluid inclusions. *Organic Geochemistry, 29*(1–3), 631–648.

Ghosh, S. K. (2003). First record of marine bivalves from the Talchir Formation of the Satpura Gondwana basin, India: Palaeobiogeographic implications. *Gondwana Research, 6*(2), 312–320.

Ghosh, S. K., & Mukhopadhyay, A. (1985). Tectonic history of the Jharia Basin, an intracratonic Gondwana basin in Eastern India. *Quarterly Journal of the Geological, Mining and Metallurgical Society of India, 57*, 33–58.

González-Vila, F. J. (1995). Alkane biomarkers. Geochemical significance and application in oil shale geochemistry. In Composition, Geochemistry and Conversion of Oil Shales (pp. 51–68). Dordrecht: Springer.

Gupta, A. (1991). Facies analysis in Barakar Formation, Ramgarh coalfield, Bihar. *Indian Minerals, 45*(3), 163–174.

Gupta, A. (1992). Reconstruction of paleoenvironment and possible ancient sea conditions: Studies from wave-ripple marks within a part of Barakar formation, Ramgarh coalfield, Bihar. *Indian Minerals, 46*(2), 133–142.

Gupta, A. (1999). Early Permian palaeoenvironment in Damodar valley coalfields, India: An overview. *Gondwana Research, 2*(2), 149–165.

Hall, P. B., Schou, L., & Bjorøy, M. (1985). Aromatic hydrocarbon variations in North Sea wells. In *Petroleum geochemistry in exploration of the Norwegian Shelf: Proceedings of a Norwegian petroleum society (NPF) conference organic geochemistry in exploration of the Norwegian Shelf held in Stavanger, 22–24 October 1984* (pp. 293–301). Dordrecht: Springer.

Hughes, W. B., Holba, A. G., & Dzou, L. I. (1995). The ratios of dibenzothiophene to phenanthrene and pristane to phytane as indicators of depositional environment and lithology of petroleum source rocks. *Geochimica Et Cosmochimica Acta, 59*(17), 3581–3598.

Hunt, J. M. (1996). *Petroleum geology and geochemistry* (p. 617). W. H. Freeman and Company.

Jarvie, D. M., Hill, R. J., Ruble, T. E., & Pollastro, R. M. (2007). Unconventional shale-gas systems: The Mississippian Barnett Shale of north-central Texas as one model for thermogenic shale-gas assessment. *AAPG Bulletin, 91*(4), 475–499.

Johns, R. B. (1986). Biological markers in the sedimentaty record. In *Methods in geochemistry and geophysics* (Vol. 24). Amsterdam: Elseiver.

Kanzari, F., Syakti, A. D., Asia, L., Malleret, L., Mille, G., Jamoussi, B., & Doumenq, P. (2012). Aliphatic hydrocarbons, polycyclic aromatic hydrocarbons, polychlorinated biphenyls, organochlorine, and organophosphorous pesticides in surface sediments from the Arc river and the Berre lagoon, France. *Environmental Science and Pollution Research, 19*, 559–576.

Krishnan, M. S. (1949). *Geology of India and Burma* (pp. 241–298).

Lijmbach, G. M. G. (1975). On the origin of petroleum. In *9th world petroleum congress, proceedings* (Vol. 2, pp. 357–369). New York: Appled Science Publishers.

Mani, D., & Kar, N. R. (2024). Emerging techniques for evaluating thermal maturity in shale gas systems. *Unconventional shale gas exploration and exploitation: Current trends in shale gas exploitation* (pp. 1–13). Springer.

Mani, D., Kar, N. R., & Kalpana, M. S. (2022). Source rock geochemistry for shale characterization. *Handbook of petroleum geoscience: Exploration, characterization, and exploitation of hydrocarbon reservoirs* (pp. 233–253). Wiley.

Mani, D., Patil, D. J., Dayal, A. M., & Prasad, B. N. (2015). Thermal maturity, source rock potential and kinetics of hydrocarbon generation in Permian shales from the Damodar Valley basin, Eastern India. *Marine and Petroleum Geology, 66*, 1056–1072.

Mello, M. R., Gaglianone, P. C., Brassell, S. C., & Maxwell, J. R. (1988a). Geochemical and biological marker assessment of depositional environments using Brazilian offshore oils. *Marine and Petroleum Geology, 5*(3), 205–223.

Mello, M. R., Telnaes, N., Gaglianone, P. C., Chicarelli, M. I., Brassell, S. C., & Maxwell, J. R. (1988b). Organic geochemical characterisation of depositional palaeoenvironments of source rocks and oils in Brazilian marginal basins. *Organic geochemistry in petroleum exploration* (pp. 31–45). Pergamon.

MH, S., Angiolini, L., & Leng, M. J. (2007). The Early Permian fossil record of Gondwana and its relationship to deglaciation: A review. In *Deep-time perspectives on climate change: Marrying the signal from computer models and biological proxies* (p. 169). London: The Geological Society.

Mishra, H. K., & Cook, A. C. (1992). Petrology and thermal maturity of coals in the Jharia Basin: Implications for oil and gas origins. *International Journal of Coal Geology, 20*(3–4), 277–313.

Moldowan, J. M., Fago, F. J., Carlson, R. M. K., Young, D. C., An Duvne, G., Clardy, J., Schoell, M., Pillinger, C. T., & Watt, D. S. (1991). Rearranged hopanes in sediments and petroleum. *Geochimica Et Cosmochimica Acta, 55*(11), 3333–3353.

Moldowan, J. M., Seifert, W. K., & Gallegos, E. J. (1985). Relationship between petroleum composition and depositional environment of petroleum source rocks. *AAPG Bulletin, 69*(8), 1255–1268.

Moldowan, J. M., Sundararaman, P., & Schoell, M. (1986). Sensitivity of biomarker properties to depositional environment and/or source input in the Lower Toarcian of SW-Germany. *Organic Geochemistry, 10*(4–6), 915–926.

Mukhopadhyay, G., Mukhopadhyay, S. K., Roychowdhury, M., & Parui, P. K. (2010). Stratigraphic correlation between different Gondwana basins of India. *Journal of the Geological Society of India, 76*, 251–266.

Mukhopadhyay, S. K. (1996). Trace fossils as palaeoenvironmental and sedimentological indices of coal bearing Gondwana sequence. *Gondwana Nine, 1*, 505–528.

Murphy, M. E., Narayanan, S., Gould, G., Lawlor, S., Noonan, J., & Prentice, D. (1972). Organic geochemistry of some Upper Pennsylvanian and Lower Permian Kansas shales: Hydrocarbons. *Bulletin (kansas Geological Survey), 204*, 19–25.

Padhy, P. K., & Das, S. K. (2013). Shale oil and gas plays: Indian sedimentary basins. *Geohorizons, 18*(1), 20–25.

Parrish, J. T. (1990). Gondwanan paleogeography and paleoclimatology. *Antarctic paleobiology: Its role in the reconstruction of Gondwana* (pp. 15–26). Springer.

Peters, K. E., & Moldowan, J. M. (1993). *The biomarker guide: Interpreting molecular fossils in petroleum and ancient sediments*.

Peters, K. E., Walters, C. C., & Moldowan, J. M. (2005). *The biomarker guide* (Vol. 2). Cambridge University Press.

Philp, P., Symcox, C., Wood, M., Nguyen, T., Wang, H., & Kim, D. (2021). Possible explanations for the predominance of tricyclic terpanes over pentacyclic terpanes in oils and rock extracts. *Organic Geochemistry, 155*, 104220.

Philp, R. P. (1985a). Biological markers in fossil fuel production. *Mass Spectrometry Reviews, 4*(1), 1–54.

Philp, R. P. (1985b). *Fossil fuel biomarkers applications and spectra*. Elsevier.

Philp, R. P., & Lewis, C. A. (1987). Organic geochemistry of biomarkers. *Annual Review of Earth and Planetary Sciences, 15*(1), 363–395.

Powell, T. G. (1984). *Developments in concept of hydrocarbon generationfrom terrestrial organic matter*. Beijing petroleum symposium, 20–24 Sept 1984, Beijing, China.

Radke, M. (1987). Organic geochemistry of aromatic hydrocarbons. *Advances in Petroleum Geochemistry, 2*, 141–207.

Radke, M. (1988). Application of aromatic compounds as maturity indicators in source rocks and crude oils. *Marine and Petroleum Geology, 5*(3), 224–236.

Radke, M., Welte, D. H., & Willsch, H. (1982). Geochemical study on a well in the Western Canada Basin: Relation of the aromatic distribution pattern to maturity of organic matter. *Geochimica Et Cosmochimica Acta, 46*(1), 1–10.

Raymond, A. (1985). Floral diversity, phytogeography, and climatic amelioration during the Early Carboniferous (Dinantian). *Paleobiology, 11*(3), 293–309.

Rontani, J. F., & Bonin, P. (2011). Production of pristane and phytane in the marine environment: Role of prokaryotes. *Research in Microbiology, 162*(9), 923–933.

Roy, J. S. (2015). *Depositional environment of Barren Measures in East Bokaro Coalfield, Bokaro District, Jharkhand*. Retrieved from www.portal.gsi.gov.in/gsiDoc/pub/cs_ebcf-bm_facies.pdf.

Roy, A. B., & Purohit, R. (Eds.) (2018). Chapter 14—Geology of the Gondwana Supergroup. In *Indian shield* (pp. 273–285). Amsterdam: Elsevier.

Rullkötter, J., Peakman, T. M., & Ten Haven, H. L. (1994). Early diagenesis of terrigenous triterpenoids and its implications for petroleum geochemistry. *Organic Geochemistry, 21*(3–4), 215–233.

Seifert, W. K., & Moldowan, J. M. (1978). Applications of steranes, terpanes and monoaromatics to the maturation, migration and source of crude oils. *Geochimica Et Cosmochimica Acta, 42*(1), 77–95.

Seifert, W. K., & Moldowan, J. M. (1986). Use of biological markers in petroleum exploration. *Methods in Geochemistry and Geophysics, 24*, 261–290.

Simoneit, B. R., & Fetzer, J. C. (1996). High molecular weight polycyclic aromatic hydrocarbons in hydrothermal petroleums from the Gulf of California and Northeast Pacific Ocean. *Organic Geochemistry, 24*(10–11), 1065–1077.

Strachan, M. G., Alexander, R., & Kagi, R. I. (1988). Trimethylnaphthalenes in crude oils and sediments: Effects of source and maturity. *Geochimica Et Cosmochimica Acta, 52*(5), 1255–1264.

Summons, R. E., & Powell, T. G. (1987). Identification of aryl isoprenoids in source rocks and crude oils: Biological markers for the green sulphur bacteria. *Geochimica Et Cosmochimica Acta, 51*(3), 557–566.

Tao, S., Wang, C., Du, J., Liu, L., & Chen, Z. (2015). Geochemical application of tricyclic and tetracyclic terpanes biomarkers in crude oils of NW China. *Marine and Petroleum Geology, 67*, 460–467.

Tissot, B. P., & Welte, D. H. (1984). *Petroleum formation and occurrence*. Springer.

Varma, A. K., Hazra, B., Mendhe, V. A., Chinara, I., & Dayal, A. M. (2015). Assessment of organic richness and hydrocarbon generation potential of Raniganj basin shales, West Bengal, India. *Marine and Petroleum Geology, 59*, 480–490.

Veevers, J. J., & Tewari, R. C. (Eds.). (1995). *Gondwana master basin of peninsular India between Tethys and the interior of the Gondwanaland province of Pangea* (Vol. 187). Geological Society of America.

Volkman, J. K. (1986). Acyclic isoprenoids as biological markers. *Biological markers in the sedimentary record* (pp. 1–42). Elseiver.

Volkman, J. K. (1988). Biological marker compounds as indicators of the depositional environments of petroleum source rocks. *Geological Society, London, Special Publications, 40*(1), 103–122.

Wakeham, S. G., Schaffner, C., & Giger, W. (1980). Poly cyclic aromatic hydrocarbons in Recent lake sediments—II. Compounds derived from biogenic precursors during early diagenesis. *Geochimica Et Cosmochimica Acta, 44*(3), 415–429.

Walters, C. C., & Moldowan, J. M. (2005a). *The biomarker guide (Vol. 1): Biomarkers and isostopes in the environment and human history*. Cambridge University Press.

Wang, A., Li, C., Li, L., Pu, R., Yang, Z., Zhu, N., & Guo, K. (2023). C20–C21–C23 tricyclic terpanes abundance patterns: Origin and application to depositional environment identification. *Frontiers in Earth Science, 11*, 1128692.

Wang, X. C., Sun, S., Ma, H. Q., & Liu, Y. (2006). Sources and distribution of aliphatic and polyaromatic hydrocarbons in sediments of Jiaozhou Bay, Qingdao, China. *Marine Pollution Bulletin, 52*(2), 129–138.

Xiao, H., Wang, T. G., Li, M., Fu, J., Tang, Y., Shi, S., Yang, Z., & Lu, X. (2018). Occurrence and distribution of unusual tri-and tetracyclic terpanes and their geochemical significance in some Paleogene oils from China. *Energy & Fuels, 32*(7), 7393–7403.

Zhang, H., Huang, H., Li, Z., Liu, M., Jiang, C., & Xu, X. (2022). Thermal stability and parameter validity of hopane series in mature

shales—A case study from Dongying Depression, eastern China. *Fuel, 315*, 123222.

Zhi-Hua, H., Hui-Xiang, L., Rullkötter, J., & Mackenzie, A. S. (1986). Geochemical application of sterane and triterpane biological marker compounds in the Linyi Basin. *Organic Geochemistry, 10*(1–3), 433–439.